Metal pollution trajectories and mixture risk assessed by combining dated cores and subsurface sediments along a major European river (Rhône River, France)

André-Marie Dendievel, Brice Mourier, Aymeric Dabrin, Hugo Delile, Alexandra Coynel, Antoine Gosset, Yohan Liber, Jean-François Berger, Jean-Philippe Bedell

Environment International 144 (2020) 106032

Contents lists available at ScienceDirect

Environment International

journal homepage: www.elsevier.com/locate/envint

Metal pollution trajectories and mixture risk assessed by combining dated cores and subsurface sediments along a major European river (Rhône River, France)

André-Marie Dendievel[a,*], Brice Mourier[a,*], Aymeric Dabrin[b], Hugo Delile[b], Alexandra Coynel[c], Antoine Gosset[a,d], Yohan Liber[a], Jean-François Berger[e], Jean-Philippe Bedell[a]

[a] Univ Lyon, Université Claude Bernard Lyon 1, CNRS, ENTPE, UMR 5023 LEHNA, F-69518 Vaulx-en-Velin Cedex, France
[b] INRAE, Centre de Lyon-Villeurbanne, UR RiverLy, F-69625 Villeurbanne Cedex, France
[c] Université de Bordeaux, UMR CNRS 5805 EPOC, F-33615 Pessac, France
[d] Ecole Urbaine de Lyon, Institut Convergences, Commissariat général aux investissements d'avenir, Atrium, 43 Boulevard du 11 novembre 1918, F-69616 Villeurbanne, France
[e] CNRS, Univ Lyon, Université Lyon 2, UMR 5600 EVS-IRG, F-69676 Bron Cedex, France

ARTICLE INFO

Handling Editor: Adrian Covaci

Keywords:
Geo-accumulation index
Geochemical baselines
Metal contamination
Pollution legacy
River sediments

ABSTRACT

In European rivers, research and monitoring programmes have targeted metal pollution from bed and floodplain sediments since the mid-20th century by using various sampling and analysis protocols. We propose to characterise metal contamination trajectories since the 1960s based on the joint use of a large amount of data from dated cores and subsurface sediments along the Rhône River (ca. 512 km, Switzerland–France). For the reconstruction of spatio-temporal trends, enrichment factors (EF) and geo-accumulation (Igeo) approaches were compared. The latter index was preferred due to the recurrent lack of grain-size and lithogenic elements in the dataset. Local geochemical backgrounds were established near (1) the Subalps and (2) the Massif Central to consider the geological variability of the watershed. A high contamination (Igeo = 3–5) was found for Cd, Cu and Zn from upstream to downstream over the period 1980–2000. This pattern is consistent with long-term emissions from major cities and the nearby industrial areas of the Upper Rhône (Geneva, Arve Valley), and Middle Rhône (Lyon, Chemical Corridor, Gier Valley). Hotspots due to Cu and Zn leaching from vineyards, mining, and highway runoff were also identified, while Pb was especially driven by industrial sources. The recovery time of pollution in sediment varied according to the metals and was shorter upstream of Lyon (15–20 years) than downstream (30–40 years). More widely, it was faster on the Rhône than along other European rivers (e.g. Seine and Rhine). Finally, the ecotoxicological mixture risk of metal with Persistent Organic Pollutants (POPs) for sediment-dwelling organisms showed a medium "cocktail risk" dominated by metals upstream of Lyon, although it is enhanced due to POPs downstream, and southward to the delta and the Mediterranean Sea. Overall, this study demonstrates the heterogeneity of the contamination trends along large fluvial corridors such as the Rhône River.

1. Introduction

Since 1980, metal pollution closely related to various human activities has been a major environmental issue in river catchments (e.g. Chamley, 2003; Deycard et al., 2014; Förstner and Salomons, 1980; Müller, 1979; Thévenot et al., 1998). In the Northern hemisphere, the highest human-induced contamination of aquatic sediments by metals occurred between 1950 and 1980 (Glorious Thirties), followed by a decreasing phase. However adjustments to this general pattern are definitely found from one country to another, associated to various times of recovery in river sediments (Callender, 2003). It could be defined as the period needed to return or evolve, upon a disturbance, into an equilibrium characterised by stable and low pollution (Brenner et al., 2004; Moore and Langner, 2012).

Historically, two main approaches were used to assess the status of contamination in river sediments based on different sampling and analysis strategies (Meybeck, 2013; Reuther, 2009). On the one hand, the regulatory monitoring was performed on stream sites by extracting and analysing subsurface sediments (< 20 cm in depth; WFD AMPS, 2004). This approach produced numerous data which varied greatly in

* Corresponding authors.

https://doi.org/10.1016/j.envint.2020.106032
Received 7 May 2020; Received in revised form 31 July 2020; Accepted 31 July 2020
Available online 26 August 2020

Nomenclature

AD	Anno Domini
AR	*Aqua Regia*
BDE-209	Penta-bromodiphenylether
BFD	Bed and Flood Deposit
BFR	Brominated Flame Retardant
DDD	Dichlorodiphenyl -dichloroethane
DDE	Dichlorodiphenyl -dichloroethylene
DDT	Dichlorodiphenyl-trichloroethane
CA	Concentration Addition
clr	Centred log-ratios
EF	Enrichment Factor
FF	Fine Fraction
GBS	Geochemical Background Sample
GC	Geographical Cluster
HBCD	Hexabromocyclododecane
HCB	Hexachlorobenzene
HCH	Hexachlorocyclohexane
Igeo	geo-accumulation Index
LOQ	Limit Of Quantification
MGB	Median-based Geochemical Background
Me	Metals
MEC	Measured Environmental Concentration
OCP	OrganoChlorine Pesticide
PCA	Principal Component Analysis
PCB	PolyChlorinated Biphenyl
PEC	Probable Effect Concentration
PNEC	Predicted No Effect Concentration
POP	Persistent Organic Pollutant
RCS	River Core Sample
RMC WA	Rhône-Méditerranée-Corse Water Agency
RQ	Risk Quotient
SPM	Suspended Particulate Matter
TE	Total Extraction
TEC	Threshold Effect Concentration
TOC	Total Organic Carbon

content and quality (variable limits of quantification, lack or late measurement of Total Organic Carbon [TOC], grain-size, and lithogenic elements). In addition, sediment monitoring was usually performed during a determined – and not always continuous – period (daily, monthly, yearly) which does not facilitate the intercomparison of the pollution between sites and rivers over time (e.g. Crane and Hennes, 2007; Dendievel et al., 2020a; Gil-Díaz et al., 2019; Heise and Förstner, 2006; Ollivier et al., 2011; Priadi et al., 2011; Tang et al., 2018). On the other hand, retrospective studies assessing temporal pollution trends are based on sediment cores collected at a specific river location where sediment regularly deposited over the last decades (reservoir, floodplain, oxbow lake). This approach employed sediment accumulation models based on radionuclides (^{137}Cs, ^{210}Pb) and on grain-size changes (induced by floods, flushes, river management) to reconstruct the pollution history. Usually, one sediment core is supposed to stand for the whole river catchment. Actually, if such an approach might be effective for short and homogeneous rivers (the Scheldt: Covaci et al., 2005; the Hong-Kong rivers: Fung and Lo, 1997; the Florida rivers: Santschi et al., 2001), however it is less relevant to identify pollution sources, temporal, and diffusion trends in large heterogeneous rivers, because depositional contexts are highly variable (e.g. Dhivert et al., 2015; Grygar et al., 2016; Vauclin et al., 2020).

A large amount of data has been – and is still – produced by these two approaches. However, synthesis works at the scale of large rivers are rather rare (Rhine River: Heise and Förstner, 2006; Seine River: Meybeck et al., 2007, 2018). Due to the data and protocols heterogeneity (sampling, dating, metal analyses), one of the main challenges to improve the understanding of long-term metal pollution trajectories and time recovery in river sediment is to find an approach to jointly analyse and interpret pollutant data from dated cores and subsurface samples together. In addition, as metal can be mixed with persistent organic pollutants (POPs), it is also important to consider both metals and POPs in terms of ecotoxicity risks (Gao-Ping River, Taïwan: Doong et al., 2008; Liao River, China: Liu et al., 2015a; Rhine, W. Europe: Heise and Förstner, 2006; St-Lawrence, Canada: Pelletier and Blais, 2018; Southern USA rivers: Santschi et al., 2001), to better evaluate the spread and degree of pollution, the risk of mixture, i.e. “cocktail effect”, and the impact on the sediments and ecosystems (Backhaus and Faust, 2012).

As a result, the objectives of this article are twofold: (1) to characterise the temporal and longitudinal complexity of metal pollution of a large and heterogeneous river since the 1960s according to the regional geochemical background variations and by using the most adapted pollution indices, and (2) to assess the pollutant contribution to the ecotoxicological mixture risk for sediment-dwelling organisms (metals and POPs) along a major European river: the Rhône from Geneva (Switzerland) to its delta (France, distance = 512 km).

2. Materials and methods

2.1. Sampling sites and chronology

2.1.1. The Rhône River: Hydrological and geological context

From the outlet of the Geneva Lake (Switzerland) to its delta (France), the Rhône River (Fig. 1) is under a complex hydrological regime which is mainly pluvial. It also integrates a snowmelt and a Mediterranean influence with major precipitations in winter, spring, and autumn (Sauquet et al., 2008). Like many long rivers, the Rhône sub-catchments present contrasting hydrological and geological characteristics developed hereafter (Bravard, 2010; Olivier et al., 2009).

In the Upper section, downstream of the Geneva conurbation (0.9 $M_{inhab.}$), the Rhône receives large amounts of fine sediments from the Arve River which consisted mainly in rock flour from glaciated areas dominated by crystalline rocks from the Prealps and the Inner Alps (Fig. 1: R1; see also Arnaud et al., 2015). Then, flowing between the Subalps and the South-Jura (limestone, molasse, moraines, and fluvio-glacial deposits), it drains the Dauphiné Lowlands accreted by fine sediments deposited by the Rhône and its tributaries, the Fier and Guiers rivers (Salvador et al., 2005; see also Fig. 1: R2 and R3). After a straight course to the north-west, the Rhône River receives a high bedload from the Ain River (calcareous sediments mainly), and passes through Lyon where it meets the Saône River (supplied by both sedimentary, detrital and crystalline areas – cf. Fig. 1: R4). After the Lyon conurbation (1.4 $M_{inhab.}$), the Rhône exceeds 1000 $m^3\ s^{-1}$ (Bravard, 2010; Thollet et al., 2018). Then, the Rhône goes southwards and its water discharge gradually increases in the Middle Rhône Valley. In this section, the river is supplied by (1) right bank tributaries from the Hercynian Massif central (granitic, metamorphic, and basaltic rocks: ca. 20% of the Middle Rhône watershed) such as the Gier, Eyrieux, Cance, and Ardèche rivers (Fig. 1: R5–R8), and by (2) left bank tributaries from the calcareous subalpine zone (40% of the Middle Rhône watershed) such as the Isère and Drôme rivers (Fig. 1), which provide large amounts of suspended particulate matter – SPM (Poulier et al., 2019). Stream sediments from right bank tributaries are Cd and Pb-rich, while left bank tributaries provide generally Cu-rich sediments (Delile et al., 2020; De Vos et al., 2006). At the transition with the Lower Rhône, the river flows into small successive sedimentary basins (Montélimar and

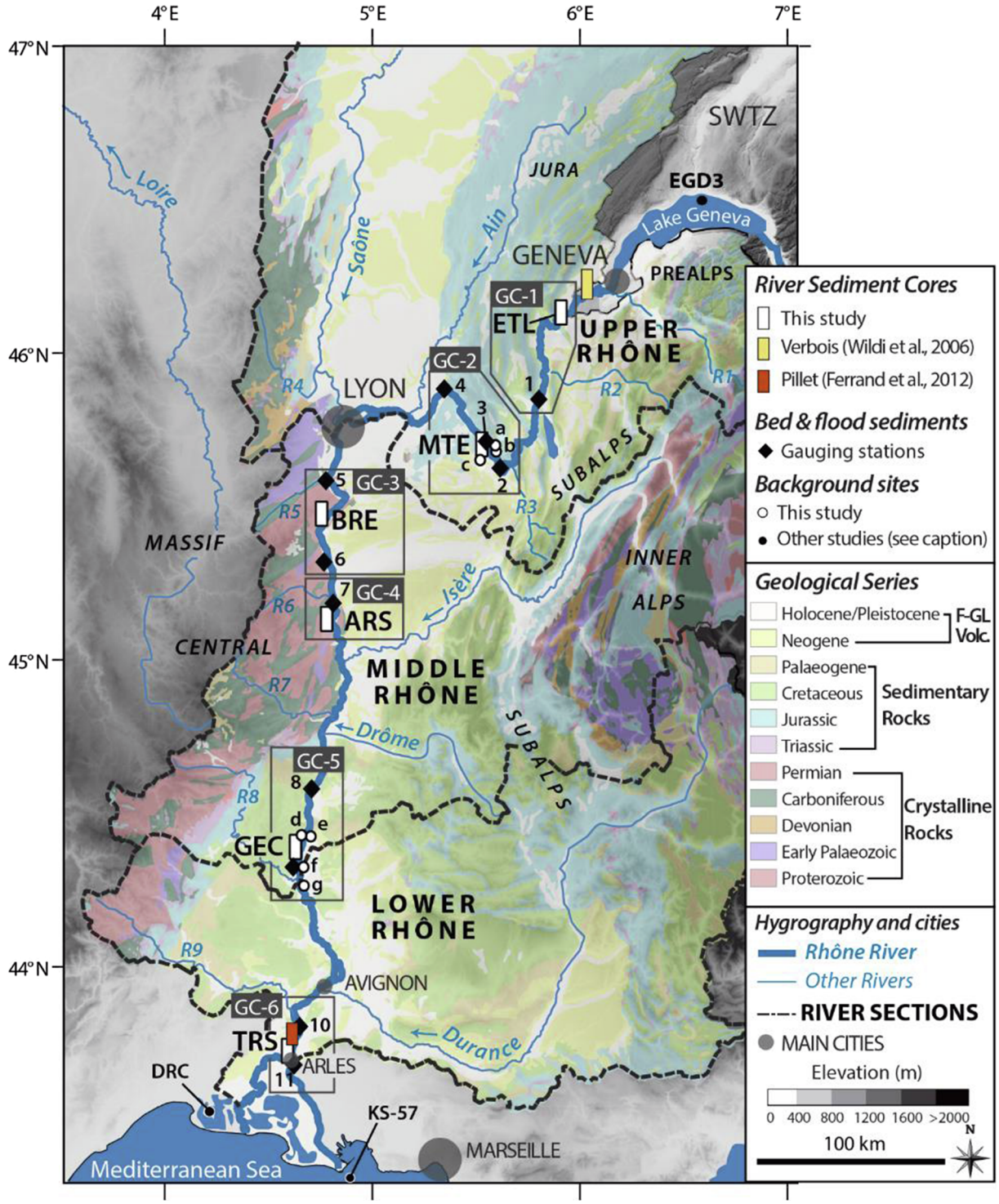

Fig. 1. Regional geology and location of sampling sites in the Rhône Valley (France). River sediment cores of this study: ETL = Gravière-des-étournels, MTE = La Morte Palaeochannel, BRE = Beurre Island, ARS = Arras-sur-Rhône dam, GEC = Grange-écrasée, TRS = Mas des Tours. Monitoring stations: 1 = Ruffieux and Culoz, 2 = Brégnier-Cordon, 3 = Brangues, 4 = St-Sorlin-en-Bugey, 5 = Chasse-sur-Rhône/Givors, 6 = Serrières, 7 = St-Vallier, 8 = Rochemaure, 9 = Pierrelatte, 10 = Beaucaire, 11 = Arles2. Geochemical background coring sites: a = EM5, b = CHCO-S2 and LMS1, c = PDC-S8, d = DZR-C3, e = DZ-1, f = LPP-C1, g = MGN-C1. Other background studies: EGD3 = Vidy Core, Geneva Lake (Gascón Díez et al., 2017), DRC = Delta Reference Core (Ferrand et al., 2012), KS-57 = Pro-Delta Core (Cossa et al., 2018). The six geographical clusters (GC) refer to the zones described in the text and in the Table 1. Geology: F = Fluvial deposits, GL = moraines and fluvio-glacial deposits, Volc. = volcanic rocks. Rivers: R1 = Arve, R2 = Fier, R3 = Guiers, R4 = Azergues, R5 = Gier, R6 = Cance, R7 = Eyrieux, R8 = Ardèche, R9 = Gard.

Tricastin floodplains). Downstream of the Donzère bottleneck, the floodplain extends and hosts some urban and industrial areas (Avignon, Arles). Finally, the Rhône River receives sedimentary inputs from the lower Durance and Gard rivers (Fig. 1: R-9), and flows into the Mediterranean Sea through a large delta (1700 $m^3\ s^{-1}$).

Since the mid-19th century, the Rhône experienced two types of water engineering associated with distinct periods. Infrastructures related to navigation and flood protection (embankments, dikes, groynes)

were implemented in the 18th and 19th centuries, while hydropower structures (weirs, dams, by-passed sections) were built during the 20th century (Bravard and Bethemont, 2018). These engineering works are present all along the river corridor. It resulted in a major reduction of the main stream width, a lower connexion with the floodplain, and the deposition of fine sediments in infrastructures and backwater areas during the last decades (Tena et al., 2020; Vauclin et al., 2019).

2.1.2. Geochemical background cores

Natural metal levels in river sediments were assessed by analysing geochemical background samples (abridged GBS hereafter) from pre-industrial cores extracted in two areas selected to represent the geology of the river catchment :

(1) In the Upper Rhône Valley, three cores from the Dauphiné Lowlands palaeomeanders were used (Fig. 1: a–c; cores CHCO-S2, EM-5, PDC-S8). A synthesis of regional fluvial dynamics dated these palaeomeanders back to the Holocene (Salvador and Berger, 2014). Seven samples were extracted from the basal sediment sequences which were highly laminated due to distal flood inputs (SI-1: A). These records could be considered representative of the erosion of the limestone, molasse and crystalline rocks from Upper Rhône Valley (Arnaud et al., 2015).
(2) At the transition between the Middle and Lower Rhône Valleys, four other cores were sampled in the Tricastin floodplain (Fig. 1: d–g; cores: DZ-1, DZR-C3, MGN-C1, and LPP-C1) where numerous palaeochannels are found next to the Berre and Ardèche rivers confluences (Bravard et al., 2008; Provansal et al., 1999). Eight layers were extracted from the bottom of the sediment sequences. Depositional conditions are similar to those from the Upper Rhône (silty laminated deposits) with a higher oxidation degree in general (SI-1: B). This second area was established to take into account the weathering of the crystalline and volcanic rocks from the Massif Central Mountains (Fig. 1).

The GBS were selected according to their content in fine-sized particles in order to facilitate the normalisation of metal concentrations according to the grainsize (i.e. clay + silt content > 60%). These layers were dated by radiocarbon (^{14}C accelerator mass spectrometry), and calibrated ("Intcal13" curve; Reimer et al., 2013) in calendar years: from Anno Domini (AD) 3 to AD 1670 for the Upper Rhône (Roman to Modern Times), and from AD 887 at least to AD 1878 for the Middle Rhône (Middle Ages–19th century AD) (Table 1). For further details about the methodology, coring locations, and dating, please refer to the related *Data in Brief* article (Dendievel et al., in press).

2.1.3. River sediment cores (1965–2011)

Six sediment cores were extracted along the Rhône by using a

Table 1
List of river cores (green), background cores (pale yellow), and gauging stations (white) used in this study. GBS = Geochemical Background Samples, GC = Geographical clusters, MS = Gauging station. The estuary distance is given in km before the "Grand Rhone Branch" estuary. The chronology is expressed in calendar years AD (Anno Domini).

River Section	GC	Sites	Type	Coordinates (WGS 1984) Lat. (N)	Long. (E)	Estuary distance (km)	Chronology	Samples (n)
Upper Rhône River	GC-1	ETL 10-02	River core	46.132	5.935	512	1993–2009	16
	GC-1	Ruffieux	MS	45.854	5.806	468	2007–2017	7
	GC-1	Culoz	MS	45.849	5.802	467	1993–2018	23
	GC-2	MTE 08-03	Core	45.702	5.554	415	1965–2007	30
	GC-2	Brégnier-Cordon	MS	45.625	5.616	429	2000–2016	8
	GC-2	Brangues	MS	45.712	5.549	416	2009–2014	6
	GC-2	St-Sorlin-en-Bugey	MS	45.883	5.347	388	1993–2018	21
	-	CHCO-S2	GBS	45.679	5.597	420	1439–1643	2
	-	EM-5	GBS	45.699	5.593	418	1394–1670	2
	-	PDC-S8	GBS	45.651	5.520	418	3–231	3
Middle Rhône River	GC-3	BRE 08-03	River core	45.476	4.782	291	1991–2008	14
	GC-3	Chasse-sur-Rhône	MS	45.581	4.781	312	1991–2018	26
	GC-3	Serrières	MS	45.318	4.767	271	2000–2017	8
	GC-4	ARS 10-02	River core	45.133	4.807	246	1977–2010	27
	GC-4	St-Vallier	MS	45.184	4.812	255	1987–2018	31
	GC-5	GEC 11-04	River core	44.390	4.656	151	1986–2011	25
	GC-5	Roche-maure	MS	44.579	4.708	176	2008–2017	6
	GC-5	Pierrelatte	MS	44.368	4.649	151	2008–2016	7
	-	DZ-1	GBS	44.424	4.704	157	1648–1878	2
	-	DZR-C3	GBS	44.428	4.659	157	1519–1682	2
	-	MGN-C1	GBS	44.202	4.709	130	1026–1633	3
	-	LPP-C1	GBS	44.324	4.669	146	887–1013 and before	3
Lower Rhône River	GC-6	TRS 12-04	River core	43.725	4.618	53	1985–2011	25
	GC-6	Beaucaire	MS	43.804	4.650	73	2000–2017	5
	GC-6	Arles2	MS	43.679	4.623	49	1987–2018	31

UWITEC corer from a boat (May 2008 to February 2011). The studied deposits were collected from six natural or artificial backwater areas: former gravel pit ("La Gravière des Etournels" – ETL), secondary branches with a downstream connection to the main stream ("La Morte" – MTE; "L'Ile du Beurre" – BRE; "Lône de la Grange Ecrasée" – GEC; "Mas des Tours" – TRS), or at the back of a dam ("Arras-sur-Rhône" – ARS). The geographical coordinates are presented in Table 1, and accurate location maps can be found in the supplementary material published by Mourier et al. (2014). These sites show a continuous deposition of sediments during high water periods and annual floods. The timing and rates of accumulation for each site were based on ^{137}Cs activity, mainly released in the atmosphere by nuclear weapon tests from 1954 to 1964, or on the Chernobyl accident in 1986 (Pinglot and Pourchet, 1995). Specific coarse deposits (mainly sands) from well-known floods or discharge events were also considered to adjust the age-depth models. Accordingly, the MTE core (Upper Rhône) has the longest record from 1965 to 2007, while ARS, GEC (Middle Rhône), and TRS cores (Lower Rhône) allow the reconstruction of the sedimentary and pollution trends from 1977 to 2011. Lastly, for the ETL and BRE cores (Upper and Middle Rhône), only the samples deposited from 1991 onwards were used due to a change of connectivity between these sites and the main channel (Mourier et al., 2014). A dataset of 1340 measures on the river sediment cores – RCS (n samples = 137) was used in this paper, including metals, TOC (Total Organic Carbon) and grain-size data (Dendievel et al., 2020b).

2.1.4. Subsurface sediment data (1987–2018)

Metal concentrations from bed and flood deposits (BFD), monitored by the Rhône-Méditerranée-Corse Water Agency (RMC WA), were integrated at the monitoring stations located nearby the coring sites. These RMC WA stations were monitored at different time-periods: since the end of the 1980s (Arles), or since the beginning of the 1990s (Culoz, Saint-Sorlin-en-Bugey, Chasse-sur-Rhône), and more recently (stations list in Table 1). This additional dataset presents 1263 measurements (n samples = 179) including metals and TOC obtained from the "naiades" website (French server for the monitoring of water and sediment quality: http://www.naiades.eaufrance.fr). Each coring site and the close monitoring stations are grouped into geographical clusters (GC hereafter). As a result, two GC are located in the Upper Rhône (GC-1 and GC-2), three in the Middle Rhône (GC-3 to GC-5) and another in the Lower Rhône (GC-6) (see Table 1 and Fig. 1 for more details).

2.2. Analytical methods

For each core, sediment samples were sliced into 1–2 cm thick-layers every 2–4 cm. A subsampling was achieved for grain-size, TOC, and metal analyses (Al, Cd, Cr, Cu, Fe, Ni, Pb, and Zn).

2.2.1. Grain-size and total organic carbon content in the cores

Grain-size was measured with a Mastersizer 2000© particle size analyser (Malvern Panalytical) mounted with a hydro SMsmall volume dispersion unit (grain-size classes: from 0.012 to 1000 μm). The contribution of the fine sediment classes (clays < 2 μm, total fine fraction < 63 μm) and distribution (e.g. median D50 and mode) were determined for each sample according to Blott and Pye (2012). For TOC, the samples were dried (0.5 g dry weight – dw), crushed and pyrolysed in an oven at 200–650 °C, before final oxidation of the residuals at 400–750 °C (Rock-Eval 6 pyrolysis; ISTO laboratory, Orléans, France). The TOC amount was expressed in % of dw, and analytical accuracy was better than 5% (Lafargue et al., 1998).

2.2.2. Metal analysis

Two protocols of extraction were performed depending on the samples. An *Aqua Regia* (AR) extraction procedure was achieved on the six river core samples (RCS) (analysis: ENTPE, UMR 5023 LEHNA). A total extraction (TE) was employed for the fresh bed and flood deposits (BFD) according to the RMC WA procedure for sediment monitoring (analysis: Drôme Department Laboratory). Finally, to have a consistent basis for the data comparison, both extraction methods were used on the geochemical background core samples (GBS) at the INRAE (TE), and at the ENTPE (AR). Precision, analytical and procedural accuracies were controlled by replicate measurements performed on certified materials in order to check digestion and analyses. Repeated measurements (triplicates) on the same samples were achieved to test repeatability (the standard errors associated to these results are provided in the linked dataset: https://doi.pangaea.de/10.1594/PANGAEA.914477 [Dendievel et al., 2020b]).

For the AR extraction (RCS, GBS), the samples (0.1 g) were dried at 105 °C for 12 h and sieved at 63 μm. They were digested with one volume of HNO_3 (2 ml of 60% Merck Suprapur for RCS; 0.5 ml of 14 M Ultrapur for GBS) and three volumes of HCl (6 ml of 30% Merck Suprapur for RCS; 1.5 ml of 12 M Ultrapur for GBS). After digestion in a microwave system (CEM 6: 110–180 °C at a pressure of 120 PSI), samples were filtrated at 22 μm by using 25 ml of distilled water. Then, metal concentrations were measured by Atomic Absorption Spectrometry (AAS) with a Perkin Elmer PinAAcle 900 T. Flame absorption was used for Cr, Pb, and Zn (standard FD T90-112; AFNOR, 1998), and a graphite furnace was employed for Cd and Cu (NF EN ISO 15586; AFNOR, 2004). Aluminium (Al) and Iron (Fe) contents were measured with an inductively coupled plasma with optical emission spectrometry ICP-OES (NF EN ISO 11885; AFNOR, 2009). The LOQs were 5 μg kg^{-1} for Cd (standard error [se] = 3%), 2 mg kg^{-1} for Cu, Cr, Ni, Pb and Zn (se = 1.5%), and 0.1 g kg^{-1} for Al and Fe (se < 5%). Accuracy was within 10% of the certified reference materials values.

For TE (BFD, GBS), samples (0.3 g) were freeze-dried and grinded in an agate mortar. They were digested in closed, previously acid-cleaned PP reactors (DigiTUBEs; SCP Sciences) by using a tri-acid treatment: 0.5 ml of HNO_3 (14 M Suprapur), 1.5 ml of HCl (12 M Suprapur), and 2 ml of HF (22 M Suprapur). The reactors were kept at 110 °C in an automatic heating block for 2 h. The dry residues were re-dissolved with 250 ml HNO_3 and 5 ml of Ultrapure water on a heating plate (100 °C during 30 min). Then, 6.5 ml of ultrapure water was added to 3.5 ml of the latter solution for the analysis: Al, Fe, Cr, Cu, Ni and Zn were analysed by ICP-OES (NF EN ISO 11885: AFNOR, 2009), and Cd and Pb by ICP-MS (NF EN ISO 17294-2: AFNOR, 2016). The LOQs were 2.5 g kg^{-1} for Al and Fe, 2.5 mg kg^{-1} for Cr, Cu, Ni and Zn, and 0.03 mg kg^{-1} for Cd and Pb.

2.3. Data treatment

2.3.1. Treatment of undetects and normalisation to grain-size

Metal concentrations were greater than the LOQs (limits of quantification), except for Cd for which 78 samples from the BFD (i.e. 25%) were lower than the LOQs (usually 0.2 mg kg^{-1}). To handle Cd left-censored data, we used a Kaplan-Meyer procedure (Helsel, 2012). This reliable method is based on counting numbers of data at and below each detected value, and computes the 95% upper confidence limit on the mean (UCL95). It decreases the number of undetected Cd values to 39 (13%).

Taking into to account the grain-size was also one of the main issues due to the high heterogeneity of the data. Indeed, potential lithogenic elements were rare, and only acquired recently (since 2010, availability: Al and Fe) and no grain-size was measured on the Rhône River BFD. On the contrary, grain-size, Al and Fe were more systematically available for RCS and GBS. As a result, we proposed three steps to integrate the grain-size control (Sun et al., 2018):

(1) After a normality check, the correlation between the potential lithogenic elements (Al and Fe) with the proportion of clays and silts (fine fraction < 63 μm) was tested by using a student test (SI-2). It showed a highly significant correlation between Al and the fine fraction for RCS and GBS, while Fe was only correlated to the fine fraction for RCS (absence of significant correlation for GBS: see SI-2). Iron (Fe)

could therefore be a reliable option to normalise the RCS, but not for the calculation of enrichment factors based on the background values. (2) Then, a correlation test between Al, Fe and the other metals was performed and revealed a significant correlation (except between Al and Pb, and regarding Fe and Cd: SI-3). Accordingly, we propose to use Al as a proxy of the grain-size content in the Rhône River sediments (see previous uses: Ferrand et al., 2012; Ollivier et al., 2011). (3) Metal concentrations were normalised by using ratios (Me/Al). However, caution must be made regarding the systematic use of Al to normalise metal values, due to the possible anthropogenic enrichment of Al in core profiles.

2.3.2. Geochemical background

The estimation of metal pollution levels requires the establishment of a geochemical background which integrates (1) natural metal levels in river sediments (i.e. geogenic origin), and (2) anthropogenic remanence inherited from past pollutions (Reimann et al., 2005; Thévenot et al., 2007). Indeed, in the Rhône watershed, archaeological and historical studies revealed long-term mining and metallurgical activities from the Roman period to the Modern Times, or even locally since the Bronze/Copper Ages (Arnaud et al., 2010; Bailly-Maître, 2010; Cauuet, 2013).

The GBS extracted from dated palaeochannel cores were used to establish local geochemical background levels. Due to the small number of analyses on GBS (n = 7–8 per site) that present non-normally distributed results, the geochemical background should be expressed as a range between the lower and upper whiskers of Tukey's boxplot (95.6%), associated to a median value (Reimann and Garrett, 2005). This median-based geochemical background (MGB) approach is useful to calculate pollution indices, and to evaluate the timing of sediment quality recovery.

2.3.3. Characterisation of pollution sources and trends by using river sediment cores and subsurface samples

A Principal Component Analysis (PCA) was carried out separately on RCS and BFD samples. The Me/Al ratios were used to avoid the grain-size effect. Then, after the removal of missing values (NA), the data was transformed by using a centred-log ratio procedure ("clr" function from the package "rgr" [v.1.1.15: Garrett, 2018] in *R* [v. 3.5.2; R Core Team, 2018]) to correct the closure effect in the data matrix (Aitchison, 1986; Tolosana-Delgado, 2012). A biplot was computed according to the PCA results and showed compositional coordinates according to the main inertia axes.

Two pollution indices – Enrichment Factors (EF) and the geo-accumulation Index (Igeo) – were tested to evaluate the degree of contamination in river sediments (e.g. Grosbois et al., 2006, 2012; Meybeck, 2013; Müller, 1986; Reimann and de Caritat, 2000). These indices were calculated based on the Upper and Middle Rhône geochemical backgrounds (MGB) according to the location of the studied sites, and estimated separately according to each extraction procedure (AR and TE). On the one hand, EFs can take into account the grain-size control by referring to the Al content (considered as a grain-size proxy). On the other hand, the Igeo comprises a safety factor of 1.5 referring to the changes of metal concentrations linked to natural variations (Müller, 1986). In addition, the Igeo can be calculated regardless of Al (which is not available for the BFD data before 2010) and provides an independent index, which is useful when Al could be influenced by anthropogenic emissions. It results in a higher number of data being used for the spatial and temporal analysis by the Igeo compared to EF and maximises the cross-checking with the river core samples (RCS).

EFs were calculated using the following equation (1):

$$EF = (Me\_sample/Al\_sample)/(Me\_MGB/Al\_MGB) \quad (1)$$

The Igeo was calculated following Müller's equation (1979) (2):

$$Igeo = Log2(Me\_sample/(1.5 * Me\_MGB)) \quad (2)$$

In these two equations, Me_sample refers to the concentration of a metal in a sample, while Al_sample is the concentration of Al in the same sample. Me_MGB is the concentration of the considered element in the regional geochemical background (MGB). The same applies to Al_MGB. The values provided by these two indices are varied from $EF < 1.5$ (absence or low metal enrichment) to $5 < EF < 20$ (significant enrichment), and from $Igeo \leq 0$ (class 0, uncontaminated) to $Igeo \geq 4$ (highly to extremely contaminated). For more details about the EF and Igeo categories, please refer to SI-4.

Igeo and EFs spatio-temporal trends were represented using *R* (v. 3.5.2; R Core Team, 2018) and the "ggplot2" package (v.3.1.1; Wickham et al., 2019). Non-parametric models were plotted based on general additive models (gam) with an appropriate degree of freedom and number of dimensions (Wood, 2019). Gam (confidence interval = 99%) were plotted according to the six geographical clusters (GC) defined above (Fig. 1; Table 1). Gam curves were used to define the time of recovery, i.e. the decay time-period between the maximal Igeo level (according to gam) and $Igeo < 1$ for each metal (i.e. uncontaminated to moderately contaminated class).

2.3.4. Ecotoxicological risk of pollutant mixture

For this research, the ecotoxicological mixture risk of pollutant in

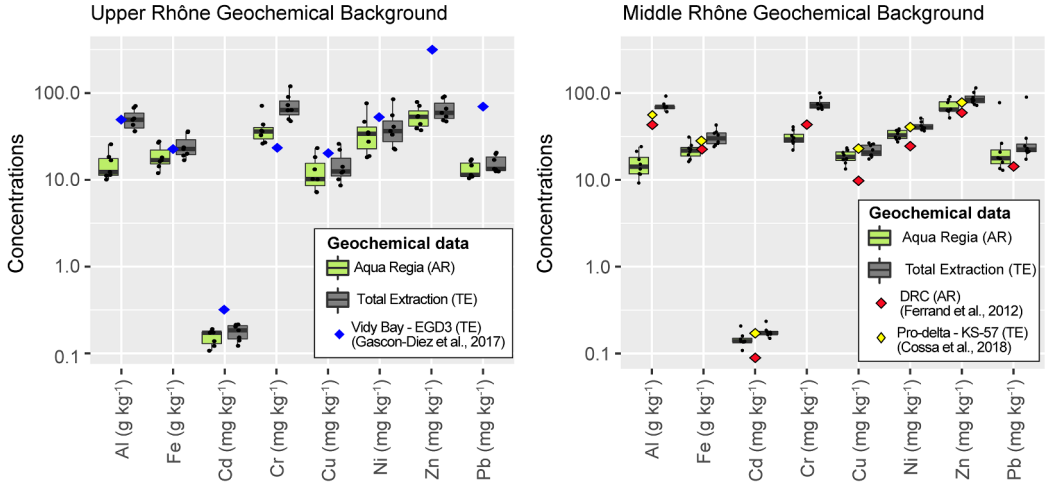

Fig. 2. Metal concentrations of background samples (GBS) after *Aqua Regia* (AR) and totally extraction (TE) protocols for the Upper and Middle Rhône. Previously published references cores are also mentioned with the associated references (see SI-2 for details).

sediments is based on both metals (Cd, Cu, Ni, Pb and Zn – data presented in this article) and on POPs from the same river cores and samples (polychlorinated biphenyls [PCBs], brominated flames retardants [BFRs], and organochlorine pesticides [OCPs]; data from Liber et al., 2019). The mixture risk is assessed according to risk quotients (for the complete list of pollutants, please refer to SI-5). The risk quotient (RQ) is a ratio between the measured environmental concentration (MEC) of each pollutant, and the corresponding $PNEC_{sed}$ (Predicted No Effect Concentration for sediment-dwelling organisms) (ECB, 2003). The use of $PNEC_{sed}$ is valuable to consider a wide range of micro-pollutants not included in the TEC and PEC (Threshold and Probable Effect Concentrations, respectively) from MacDonald et al. (2000a), such as HCHs, HCB, and BDE-209 (ECB, 2001). Current reference values for $PNEC_{sed}$ are available online at https://substances.ineris.fr/fr/. For PCBs, in the absence of a robust PNEC, we refer to the lowest sediment effect concentration provided by MacDonald et al. (2000b). Finally, RQ for each pollutant was summed to estimate the global risk of mixture based on the Concentration Addition (CA) model which assumes a similar mode and site of toxic action of all pollutants on sediment-dwelling organisms (Backhaus and Faust, 2012; Norwood et al., 2003; Smith et al., 2003). Mixture risk quotients were calculated with the following equation (3):

$$RQ_{Mix} = \Sigma(MEC_{i,x}/PNEC_{sedi}) \quad (3)$$

where RQ_{Mix} is the sum of all RQ. RQ for each pollutant is based on $MEC_{i,x}$, which is the Measured Environmental Concentration of the pollutant i on the site × (mg kg^{-1} dw), and on $PNEC_{sed\ i}$ according to the Equilibrium Partitioning (mg kg^{-1} dw). RQ_{Mix} scale is log10-based from $RQ < 1$ for a negligible risk to $100 < RQ < 1000$ which corresponds to a high risk (Gosset et al., 2020; Perrodin et al., 2012).

3. Results

3.1. Local geochemical backgrounds

A local geochemical background was established for each river section for both TE and AR extraction procedures (Fig. 2). The results are synthesised in Table 2 (for details about individual samples, please refer to Dendievel et al., in press). TE results are generally exceeding the AR values, because TE procedure extracts metal from the crystal lattice while metal concentrations obtained after an AR procedure represents, more or less, the bio-accessible part for aquatic organisms.

Despite a large chronology of sediment deposition (Fig. 1), the Upper and the Middle Rhône MGB display relatively close metal medians and ranges, and similar grain-size proportions (Fig. 2; Table 2). Nonetheless, Cu, Pb, and Zn generally present lower levels in the Upper Rhône than in the Middle Rhône (Fig. 2). These differences can be explained by the local geology and the particle eroded from the crystalline Massif Central Mountains and transported to the Middle Rhône Valley (Fig. 1). A higher level in Al and Fe in the Middle Rhône GBS is reported and could be linked to a higher oxidation state of the cores. Finally, there was no significant difference between Cd, Cr, and Ni.

The values defined for these two MGBs differ from the Upper Continental Crust, which is enriched in Cr, Cu, or Ni and have a lower level of Cd (after Rudnick and Gao, 2014; see Table 2). We preconise the use of local and adapted values – such as MGBs – to do not underestimate the importance of contamination for these metals. At a more regional scale, other geochemical background values were previously published for the Upper Rhône from the Geneva Lake (Vidy Bay, EGD3 core: Gascón Díez et al., 2017), for the Lower Rhône in the delta (DRC: Ferrand et al., 2012) and pro-delta (KS-57: Cossa et al., 2018). In the Upper Rhône, the Al content of the MGB is very close to the EGD3 basal layers (< 2% of divergence), and Cr, Ni, and Cu are within the same ranges. However, for Zn and Pb, the EGD3 base highly exceeds the Upper Rhône MGB (by 81% and 82%, respectively), most certainly due to contaminated sediments deposited since the 1920s in the Vidy Bay as hypothesised by Gascón Díez et al. (2017) and Monna et al. (1999). The Upper Rhône MGB is also less concentrated in Cu, Ni, Pb and Zn than the geochemical background provided by Vernet and Viel (1984) for the total Geneva Lake (Table 2). In the Middle/Lower Rhône area, major divergences are found for Al which is 74% higher in the DRC core. On the contrary, it appears 30% lower in the KS-57 core (Table 2). The other metals from DRC and KS-57 also present some differences with the Middle Rhône MGB (from 58% for Cr or Cu to 20–30% for Ni, Pb, or Zn), which might be due to the depositional context. Indeed, DRC and KS-57 cores were extracted from deltaic and pro-deltaic areas where physical factors (e.g. salinity) and geochemical processes (e.g. organic matter degradation) in the river-delta continuum can modify metal concentrations in sediments (Fig. 2; Table 2).

Table 2
Local geochemical background values and ranges, grain-size and organic content for the Upper and Middle Rhone background samples. Extraction methods (Ext.): AR = *Aqua Regia* and TE = Total Extraction. FF = fine fraction (< 63 µm). Med = Median.

Location	Ext.	Reference	Clay (%)	FF (%)	TOC (%)	Trace Metals (mg kg^{-1})							Major Metals (g kg^{-1})	
							Cd	Cr	Cu	Ni	Pb	Zn	Al	Fe
Upper Rhône	AR	This work	5.0	89.6	2.6	**Med**	**0.17**	**36.1**	**10.2**	**33.9**	**11.4**	**53.2**	**12.3**	16.8
						range	0.06–0.24	14–56	0–26	0–68	4–22	10–95	2–27	5–33
	ET					**Med**	**0.18**	**63.8**	**12.5**	**36.5**	**13.4**	**59.1**	**49.2**	22.63
						range	0.05–0.30	19–119	1–29	0–78	4.5–27	12–117	10–89	5–45
EGD3 – Vidy Bay		Gascón Díez et al., 2017		ca. 85	≈1		0.45	26	22.7	56	73	304	50	22.6
Geneva Lake		Vernet and Viel, 1984					0.2	70	30	50	30	60		
Middle Rhône	AR	This work	5.1	81.4	0.9	**Med**	**0.14**	**29.3**	**18.4**	**32.7**	**17.7**	**64.6**	**14.2**	21.7
						range	0.12–0.17	17.4–43	10.3–27.4	19.3–47.6	5.0–32.6	37.7–104.4	1.9–28	12–31
	ET					**Med**	**0.17**	**71.6**	**20.7**	**40.1**	**22.3**	**83.7**	**69.2**	30.1
						range	0.15–0.20	50–95	10–34	31–51	14–33	55–115	59–78	13–48
DRC – Rhône Delta	AR	Ferrand et al., 2012					0.08	44.6	9.96	25.1	14.6	61.3	44.4	22.4
KS-57 – Rhône Pro-Delta	ET	Cossa et al., 2018			≈0.5		0.17	70.23	23.54	41.82	22.31	80.57	55	28
Upper Conti-nental Crust		Rudnick and Gao, 2014					0.09	92	28	47	17	67		

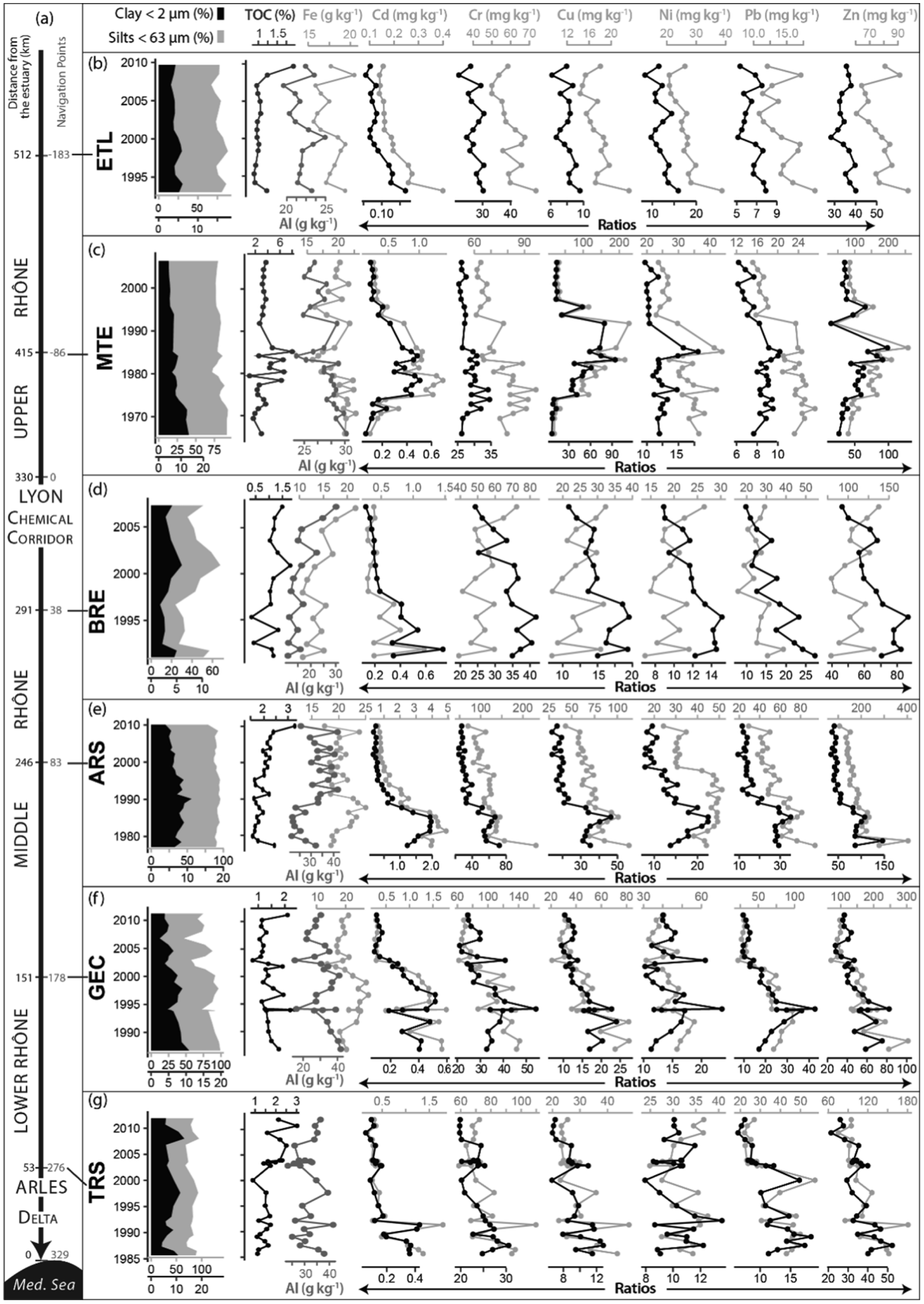

Fig. 3. Vertical profiles of grain-size, Total Organic Carbon (TOC, %), metal concentrations (light grey lines) and Me/Al ratios ($\times 10^{-4}$; black lines) for the studied river sediment core. (a) Schematic representation of the Rhône with distances in kilometres before the estuary of the "Grand Rhône" branch, and as Kilometric Points (PK) for navigation (0 = Lyon, negative PK = upstream, positive PK = downstream). The sediment cores are organised, top to bottom, from the Upper Rhône to the Lower Rhône. (b) ETL core, (c) MTE core, (d) BRE core, (e) ARS core, (f) GEC core, (h) TRS core.

3.2. Historical records of metal in sediment cores

Vertical profiles of grain-size, TOC, metal concentrations and Al normalised concentrations (Me/Al) are shown in Fig. 3. The most important metal concentrations and ratios are recorded from 1977 to the beginning of the 1990s, especially on the Middle Rhône section. The ARS site presents the highest Cd/Al, Cr/Al and Zn/Al ratios (respectively: 2, 80, and 150 $\times 10^{-4}$) and concentrations (up to 4.9, 231, and 403 mg kg^{-1}, respectively). Both ARS and GEC sites also presents the maximal ratios for Ni/Al (ca. 20 $\times 10^{-4}$), and Pb/Al (ca. 35 $\times 10^{-4}$). On the opposite, Cu highest ratios ($> 90 \times 10^{-4}$) and values (i.e. $>$ 200 mg kg^{-1}) are found at MTE in the Upper Rhône (1983–1991), but rather high Cu/Al ratios are also recorded at ARS during the 1980s (Fig. 3).

In the Upper Rhône (downstream of Geneva), the ETL core covers a 16-year long period (1993–2008). It presents a stable particle size distribution (76 ± 3.5% of fine sediments, i.e. < 63 µm) and low carbon content (0.9–1.9%). Me/Al ratios and concentrations show weak variations along the core (Fig. 3). Only the Cd/Al record presents a temporal decrease which underlines a gradual quality recovery since 1995 (ratio: 0.16–0.07 $\times 10^{-4}$). Regarding sediments quality guidelines, all metals are below the French regulatory level S1 for river sediments (JORF, 2006) and mostly below the TEC (MacDonald et al., 2000a).

Further downstream, the MTE core (1965–2007) is dominated by FF (81 ± 3.7%), but clay proportions decrease towards the top (from 40 to 20%). Me/Al ratios and concentrations show analogous patterns (Fig. 3c). Median TOC is about 3.3%, while the 1978–1991 interval has a variable organic content (1.1–8%). During this period, all metals are relatively high, especially Cu (as mentioned above). Its maximal values surpasses both the French S1 threshold for Cu (100 mg kg^{-1}: JORF, 2006), and reaches the PEC_{Cu} (150 mg kg^{-1}) from MacDonald et al. (2000a). All metals show a declining trend to low and stable values only at the end of the 1990s.

The BRE core (1991–2008) is downstream of Lyon's conurbation, in an area supplied by the Saône and the Gier rivers (Middle Rhône Valley, Fig. 1). The sediment core presents a stable TOC (1.2 ± 0.2%) (Fig. 3d). The core remains around 43 ± 7.7% of FF while the Al content increases with the core (from 11 to 30%). It could be explained by the erosion of slopes and soils from the right bank of the Rhône River, which derived from granitic rocks enriched in sillimanite ($Al_2O(SiO_4)$). Thereafter, Me/Al ratios showed a decreasing trend for all metals from 1991 to 2008, while concentrations quite low (i.e. under PEC).

Downstream, the ARS core (1977–2010) shows a stable distribution of both FF (91 ± 1.8%) and TOC (1.9 ± 0.3%). This long record displays high Me/Al ratios from 1977 to 1985, for Cd, Cu, Cr, and Ni (as described above, Fig. 3e). A decreasing trend occurs since 1985, and low and stable levels are firmly established after 1996. The maximal ratios and values regarding these metals are impressive and exceed the PEC / S1 in particular for Cd. Pb and Zn are also high, but lower than S1 and PEC.

The studied archive at GEC (1986–2011) is characterised by fine (82 ± 9%) and organic-poor sediments (1.3 ± 0.2%). Metal concentrations are medium to high, especially for Ni and Pb (highest ratios and values), and usually decrease to lower concentrations after the 1990s (Fig. 3f).

Finally, the TRS core (Lower Rhône) was retrieved upstream of the delta, north of Arles, in an area supplied by the Durance and the Gard rivers (Fig. 1). This record (1985–2012) is rather fine (81 ± 5%) and organic-poor (1.6 ± 0.3%). Despite changes in Al (20–40%), a parallel is observed between Me/Al and metal concentrations (Fig. 3g). A decreasing trend is obvious in Al/Me ratios from 1985 to 2012 with concentrations usually below S1 or TEC, and lower than in the GEC core (Fig. 3f).

3.3. Data combination, metal contamination and sediment recovery trends along the Rhône from 1965 to 2018

The PCA highlights distinct patterns for river core sediments (RCS) from 1965 to 2010 (Fig. 4A). The axes 1 and 2 represent 57.5% and 30.1% of total variance, respectively. The axis 1 is mainly driven by Cu and Cd (positive values): all the ARS record (GC-4) presents a Cd enrichment, and the MTE samples older than 1990 (GC-2) are clearly influenced by a Cu anomaly on the bottom right of Fig. 4A. The most recent MTE samples are close to the composition of ETL (GC-1), with a higher proportion of Ni and Cr (negative values of axis 1). The axis 2 is mainly driven by Cu (negative side) and Pb on the other side (positive). In the middle, the compositions from BRE, GEC and TRS are a mix of influences from axes 1 (negative) and 2 (positive) corresponding to Cr, Ni, and Pb variables.

The PCA of BFD Me/Al ratios (2010–2018) could be also described according two axis, representing more than 90% of inertia (Fig. 4B). Based on axis 1 (77.2%), two groups are observed with positive (GC-1 and GC-6), or negative values most influenced by Cd (GC-2 to GC-5). For the axis 2 (13.1%), two others groups are highlighted with (1) on

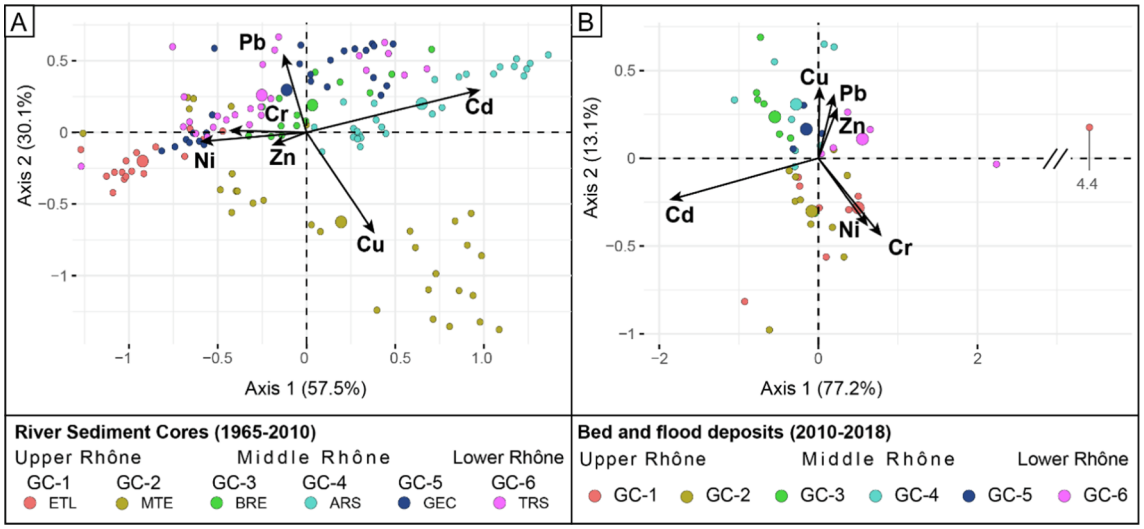

Fig. 4. Principal Component Analyses (PCA-biplots) performed separately for (A) samples from river sediment cores (n = 137) and (B) for bed and flood deposit samples (n = 78). GC refers to the geographical clusters defined in the text. The bigger circles are the centroids of the data.

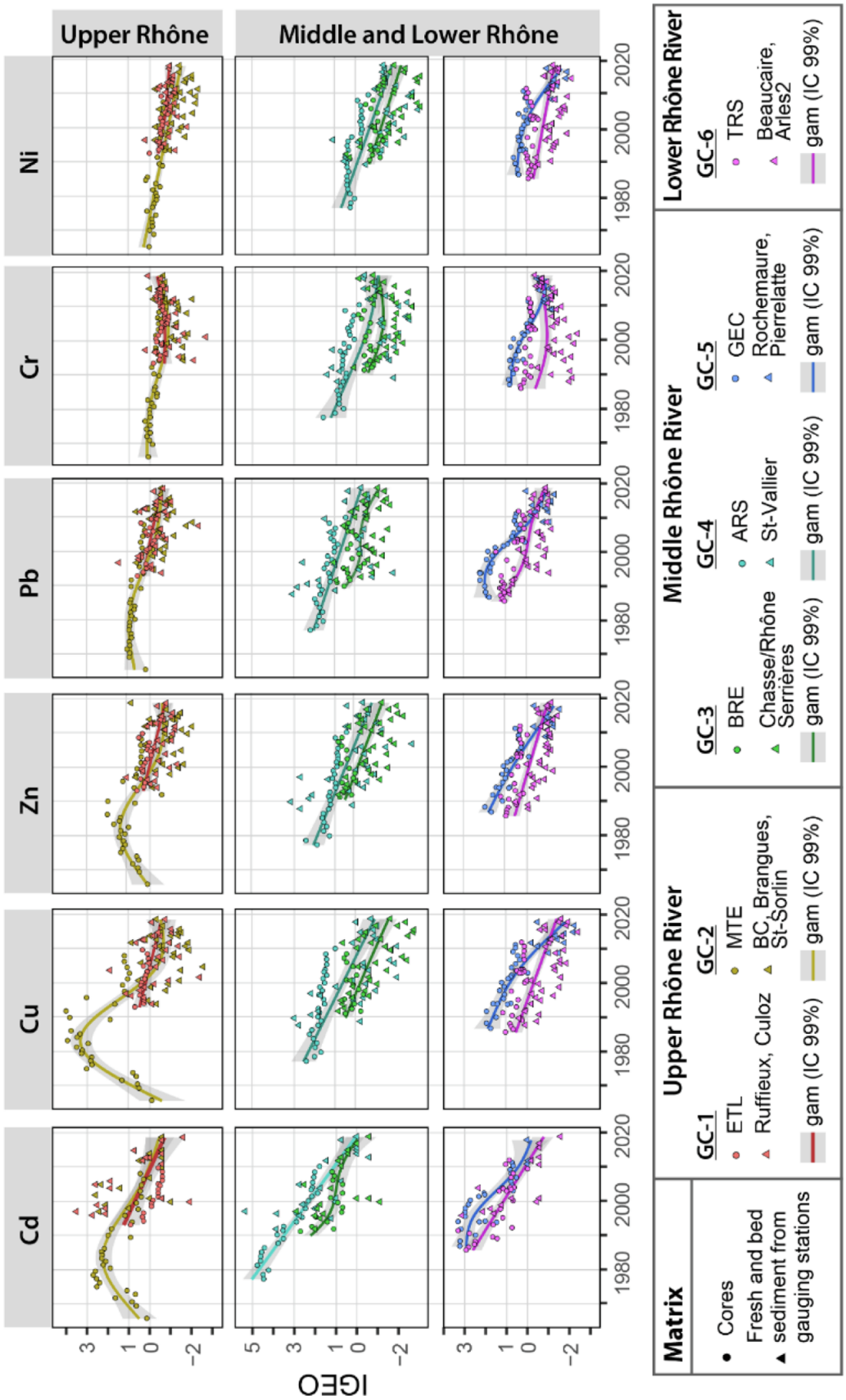

Fig. 5. Igeo changes along the Rhône River since 1965. Temporal trends are based on both sediment cores (ETL, MTE, BRE, ARS, GEC, and TRS cores) and sediment monitored at gauging stations (full names are cited, except for BC = Brégnier-Cordon). GC = Geographical Clusters defined in the text.

Table 3
Igeo and EFs values for the studied geographical clusters (GC) along the river sections (RS). EF and Igeo in bold represents moderate to significant (*) pollution of the sediment.

Metal			Cd						Cu					
Period			1965–79		1980–99		2000–18		1965–79		1980–99		2000–18	
River Section	GC		Igeo	EF	Igeo	EF	Igeo	EF	Igeo	EF	Igeo	EF	Igeo	EF
Upper Rhône	**GC-1**	Median	–	–	0.7	0.9	−0.4	1	–	–	0.3	1	−0.1	1.1
		Range	–	–	−1.9–3.5	0.6–1.2	−1.6–2.6	0.4–3	–	–	−0.2–1.1	0.9–1.2	−2.4–1.9	0.7–2.5
	GC-2	Median	**1.7**	**1.7**	**1.9**	**2.2**	0	1.4	1.3	1.5	**2.4***	**6.6***	−0.6	1.5
		Range	0.2–2.7	0.5–3.6	−1 to 2.4	0.9–3.5	−0.6 to 2.6	0.8–3.9	−0.1 to 3.3	0.8–5.9	−0.9 to 4	1.5–11.4	−2.5 to 1.2	0.8–4.5
Middle Rhône	**GC-3**	Median	–	–	**1.7**	**2.9**	0.7	**2.5**	–	–	0.2	1.3	−0.7	1.2
		Range	–	–	−1.1 to 2.9	1.8–10.6	−0.6 to 2.5	1.1–6.1	–	–	−1 to 0.9	0.8–2.1	−2.7 to 0.7	0.6–5
	GC-4	Median	**4.5***	**14.7***	**3.5***	**6.3***	**1.7**	**2.5**	**2***	**2.5**	**1.8**	**1.6**	−0.3	1.5
		Range	4.2–4.5	12.5–15.9	1–5.3	2.7–20.1	−0.6 to 2.7	1.7–8.7	1.7–2.4	2.4–2.7	−0.9 to 3	1.3–3.6	−1.9 to 1.6	0.5–3.8
	GC-5	Median	–	–	3	4.2	0.8	1.4	–	–	1.4	1.3	−0.1	0.9
		Range	–	–	1.5–3.3	1.9–5.3	0–2.7	0.9–4.6	–	–	0.8–2	1–1.9	−2.3 to 1.2	0.7–3.3
Lower Rhône	**GC-6**	Median			**1.7**	**2.7**	0.7	1.2			0.1	0.8	−0.7	0.7
		Range			−0.4 to 3.3	1.1–4.4	−1.6 to 2.3	0.5–3.5			−1.5 to 1.2	0.6–1	−2.4 to 0.5	0.5–2.9

Metal			Pb						Zn					
Period			1965–79		1980–99		2000–18		1965–79		1980–99		2000–18	
RS	GC		Igeo	EF	Igeo	EF	Igeo	EF	Igeo	EF	Igeo	EF	Igeo	EF
Upper Rhône	**GC-1**	Median	–	–	0.3	0.8	−0.3	1.1	–	–	0.3	0.9	−0.4	1
		Range	–	–	−0.6 to 1.5	0.7–0.9	−2.3 to 0.4	0.6–2.3	–	–	−1 to 1.1	0.8–0.9	−1.3 to 0.5	0.7–1.8
	GC-2	Median	1	1	0.6	0.9	−0.5	1.4	0.8	0.9	0.7	1.4	−0.7	1.1
		Range	0.2–1.1	0.8–1	−0.7 to 1	0.7–1.1	−2 to 0.7	0.7–3.9	0.1–1.5	0.6–1.5	−1.4 to 2	0.3–2.4	−2 to 0.9	0.7–3.8
Middle Rhône	**GC-3**	Median	–	–	0.1	1.5	−0.5	1.4	–	–	0.4	1.5	−0.5	1.4
		Range	–	–	−1.2 to 1.1	0.7–2.8	−1.6 to 0.6	0.7–3.2	–	–	−1.5 to 0.9	1.1–2.6	−2.2 to 0.9	0.9–3.6
	GC-4	Median	**1.9**	**2.3**	**1.5**	**1.5**	0.3	1.2	**1.9**	**1.9**	1.3	1.2	−0.1	1
		Range	1.6–2.2	2.2–2.4	−1.7 to 3.1	0.9–2.8	−0.6 to 1.5	0.8–3.2	1.3–2.4	1.9–3.2	−0.9 to 3.1	0.9–2.4	−2.6 to 1	0.8–4.1
	GC-5	Median	–	–	**2**	**1.9**	0.1	1.2	–	–	1.2	1.3	−0.2	1
		Range	–	–	1.7–2.3	1.4–3.4	−1.3–1.9	0.8–3.5	–	–	0.8–2	0.9–1.8	−1.5 to 1.1	0.6–2.3
Lower Rhône	**GC-6**	Median	–	–	0.8	1.1	−0.1	1.2	–	–	0.4	0.9	−0.5	0.9
		Range	–	–	−1 to 1.3	0.8–1.5	−1.2 to 1.5	0.5–3.3	–	–	−1.2 to 1.3	0.7–1.2	−1.4 to 0.5	0.5–2.4

Metal			Cr						Ni					
Period			1965–79		1980–99		2000–18		1965–79		1980–99		2000–18	
RS	GC		Igeo	EF	Igeo	EF	Igeo	EF	Igeo	EF	Igeo	EF	Igeo	EF
Upper Rhône	**GC-1**	Median	–	–	−0.5	1	−0.6	1	–	–	−0.5	0.5	−0.9	0.8
		Range	–	–	−2.1 to 0.2	0.9–1	−2.7 to 0.1	0.7–2.2	–	–	−1.2 to 0.2	0.4–0.6	−1.8 to −0.4	0.3–1.8
	GC-2	Median	0	1	−0.3	1	−0.7	1.2	−0.1	0.4	−0.5	0.4	−1.3	0.8
		Range	−0.1 to 0.2	0.9–1.2	−1.6 to 0.1	0.9–1.1	−2 to 0	0.9–2.4	−0.3 to 0.1	0.4–0.5	−1.7 to 0.2	0.4–0.7	−2.3 to −0.3	0.4–2.1
Middle Rhône	**GC-3**	Median	–	–	−0.8	2	−1.2	1.6	–	–	−0.9	0.6	−1.6	0.7
		Range	–	–	−2.2 to 0.1	1.2–2.6	−2.6 to −0.1	0.5–3.4	–	–	−2.1 to 0.5	0.4–0.9	−3 to −0.4	0.3–1.5
	GC-4	Median	1	**2.8**	0.7	1.8	−0.7	1.3	0.3	0.7	0.4	0.7	−1.3	0.4
		Range	0.6–1.6	2.7–3.5	−1.8 to 1.4	1.4–3.3	−2.5 to 0.6	0.3–1.9	0.1–0.3	0.6–0.8	−2.3 to 1.1	0.3–1	−2.9 to 0	0.3–1.6
	GC-5	Median	–	–	0.7	1.8	−0.4	1.3	–	–	0.4	0.6	−0.5	0.7
		Range	–	–	0.2–0.9	1.3–2.6	−1.4 to 0.7	0.9–2.3	–	–	0.1–0.7	0.5–1	−1.9 to 0.4	0.4–2.1

(*continued on next page*)

Table 3 (*continued*)

Metal			Cd						Cu					
Period			1965–79		1980–99		2000–18		1965–79		1980–99		2000–18	
River Section	GC		Igeo	EF	Igeo	EF	Igeo	EF	Igeo	EF	Igeo	EF	Igeo	EF
Lower Rhône	**GC-6**	Median	–	–	−0.5	1.3	−0.5	1.2	–	–	−0.4	0.5	−0.9	0.5
		Range	–	–	−2.2 to 0.5	1–1.5	−2.4 to 0.7	1–2.3	–	–	−1.9 to 0.1	0.4–0.6	−2.1 to 0.1	0.3–2.3

the negative side, the Ni and Cr influence on the recent deposits of GC-1 and GC-2 (Upper Rhône), and (2) on the positive side, the Cu, Pb, and Zn influence on the sediments from GC-3 to GC-6. The BFD PCA (Fig. 4B) offers some similarities and a continuous trend with the most recent deposits of the RCS (Fig. 4A). Indeed, the GC-2 samples present a gradual change from Cu (major enrichment/pollution) to Cr and Ni (geogenic). At south, the same is observed for GC-4 with a change from Cd-enriched sediments to a mix of Cu, Pb, and Zn at the vicinity of the Hercynian Massif Central (right bank inputs). These changes underline the heterogeneity of metal inputs along this large and heterogeneous European river.

The use of EFs and Igeo allow to reconstruct spatial and temporal trends of metal contamination from 1965 to 2018 by combining and modelling (gam) data from river core sediments (RCS) and bed/flood deposits (BFD; Fig. 5). EFs and Igeos variations are summarised in Table 3: these two indices present similar changes over space and time. However, EFs are based on a lower number of samples (n = 209) than the Igeo (n = 316, except for Cd for which n = 235) because the Al data – needed for EFs – is only available on BFD since 2010, which limits the analysis. Thus, in our study, the Igeo provides the best compromise between availability and quality to model metal pollution trajectories using both BFD (subsurface samples) and RCS (dated cores). It should be noted that this combined approach – which takes into account analytical results of different nature – must be used prudently, especially due to the low reliability of subsurface samples data derived from past monitoring activities (already mentioned by Thomas and Meybeck, 1996).

Among the studied metals, Cd and Cu have the highest median Igeo (2–4.5) and EFs (6.3–14.7) corresponding to a moderate to significant pollution and enrichment (Table 3). The Cd and Cu spatio-temporal pattern presents an increase during the 1970–1990s in the Upper Rhône (GC-1 and GC-2), and a regular decrease since the end of the 1980s in the Middle and Lower Rhône (GC-3 to GC-6; Fig. 5). At a lower level, Zn presents similar variations even if the contamination remained at moderate levels (Igeo classes 2 and 3; EF = 1.5–3.2).

In more details, in the Upper Rhône (GC-1 and GC-2), an increase in Igeo and EFs is observed for Cd, Cu, and Zn from 1965 to the 1990s. A heavy contamination is found for Cu between 1975 and 1990 ($Igeo_{Cu}$ = 3–4), while Cd and Zn were moderately to heavily polluted ($Igeo_{Cd}$ = 2.2–2.8; $Igeo_{Zn}$ = 1–2.3). Sporadic Cd contamination continued during the 1990s (Igeo = 2.7–3.5). Then, both Igeo and EFs decreased to less than 1 and 1.5 respectively after 1995–2005 due to a lack or a low contamination (Fig. 5; Table 3). The recovery of the sediment quality occurred earlier for Zn (during the 1990s) than for Cu and Cd (during the 2000s). Finally, Igeo values were ≤ 0 during the two last decades. In the Middle and the Lower Rhône, a general regression occurred for Cd, Zn, and Cu since the late 1970s and 1980s. At that time, a major enrichment in Cd was observed ($Igeo_{Cd}$ > 3–4; EF median = 14.7). Then, it regularly decreased until the 2000s, when a moderate level of contamination was reached ($Igeo_{Cd}$ < 2; Fig. 5), before a final decrease to non-polluted levels during the last decade ($Igeo_{Cd}$ ≤ 0). The Cu and Zn Igeos were lower and decreased, for both metals, from 3.2 (Middle Rhône) and ca. 1 (Lower Rhône) during the 1980s, to became ≤0 in the 2000s. Thus, the time of recovery for these three pollutants was longer in the Middle and Lower Rhône (ca. 30 years) than in the Upper Rhône (15–17 years).

The lead (Pb) presents a dual geo-accumulation pattern (Fig. 5; Table 3): (1) in the Upper Rhône, an absence or a very low enrichment is found (Igeo < 1 and an EF < 1.4); (2) in the Middle and Lower Rhône, the $Igeo_{Pb}$ reaches 2–3.1 (medium to highly polluted), where local anthropogenic inputs are suspected. Then, it decreased to uncontaminated levels in the late 1990s which corresponds to a recovery time comprised between 10 and 20 years.

Finally, a low geo-accumulation is found for Cr and Ni everywhere along the Rhône river (Fig. 5). For instance, the Igeo varied from < 1 in the 1970s to −2 nowadays in the Upper Rhône, and from < 1 in the

late 1980s and 1990s, to < −2 today in the Middle and Lower Rhône. Only the ARS/St-Vallier area (GC-4; Middle Rhône) displays a moderate $Igeo_{Cr}$ (> 1) at the connection with right bank tributaries coming from the Massif Central foothills. Moreover, Cr and Ni in the Rhône sediments are close to the geochemical background reference (Fig. 2 and Table 2).

4. Discussion

4.1. Assessment of anthropogenic metal sources along the Rhône and comparison with other European rivers

The identification of the main historical factors that influence the spatial and temporal trend of pollution (sources, economic developments, regulations) will be discussed for each metal element along the Rhône River, and compared to other Western European rivers.

4.1.1. Chromium (Cr) and nickel (Ni)

On one hand, Cr and Ni present low Igeos and EFs in the Upper Rhône Valley since the 1960s (Fig. 5). Currently, these rather stable indices suggest a geogenic source for Cr and Ni, which could come from the Inner Alps crystalline formations, weathered and eroded by the Arve and the Fier rivers for instance (Fig. 1). On the other hand, an enrichment in Cr and Ni was recorded in the Middle Rhône Valley in the 1970–1990s, before to decrease (Fig. 5; Table 3). This pattern indicates a local decrease of anthropogenic emissions (chemical industries, surface coating) or a lower delivery in Cr and Ni by the SPM of the right bank tributaries of the Rhône (afforestation, sediment discontinuity). Left bank tributaries coming from the Western Alps could also be involved such as the Isère SPM which are Cr and Ni-rich (Delile et al., 2020). Finally, the current Igeo values are very low for Ni and Cr (< 0) and indicate a good status of the Rhône sediment quality regarding these metals.

The Rhône pattern for Ni and Cr contrasts with the historical trajectory of some European rivers, such as the Seine, the Rhine, and their tributaries, which present moderately to heavily contaminated sediments due to (1) Cr, and (2) Ni, in order of magnitude (Fig. 6; Heise and Förstner, 2006; Le Cloarec et al., 2011). An increase from upstream to downstream is evidenced along these rivers in the 1960s and 1970s. This pollution could be related to the use of these metals for stainless steel or chemical products, surface coating, refractory purposes, and tanneries (Le Cloarec et al., 2011). On the contrary, their evolution on the Rhône presents some similarities with the Loire, the Lot–Garonne Continuum and the Thames where no particular pollution concern was highlighted for Cr and Ni (Grosbois et al., 2012; Vane et al., 2020).

4.1.2. Cadmium (Cd)

Heavily to extremely Cd polluted sediment was reported in the Dam of Verbois, in the Upper Rhône in the 1960s and 1970s (Igeo ca. 4; based on the works of Wildi et al., 2006, 2004). This site is less than 10 km downstream of the Geneva conurbation and just after the meeting point with the Arve Valley, where polluting electronic manufacturing, pigment and metal coating facilities are found (Halitim-Dubois, 2019). These multiple industrial sources could release and diffuse Cd downstream towards GC-1 and GC-2, where an $Igeo_{Cd}$ > 3 was calculated (MTE area) from 1977 to 1996 (Fig. 6).

Synchronously, the highest levels of pollution for Cd ($Igeo_{Cd}$ up to 4.5) were found in 1981–1996 in the Middle Rhône Valley (GC-3 and GC-4), downstream of Lyon where various sources may have been involved (Fig. 6). Indeed, Cd could be released during the extraction of Cu

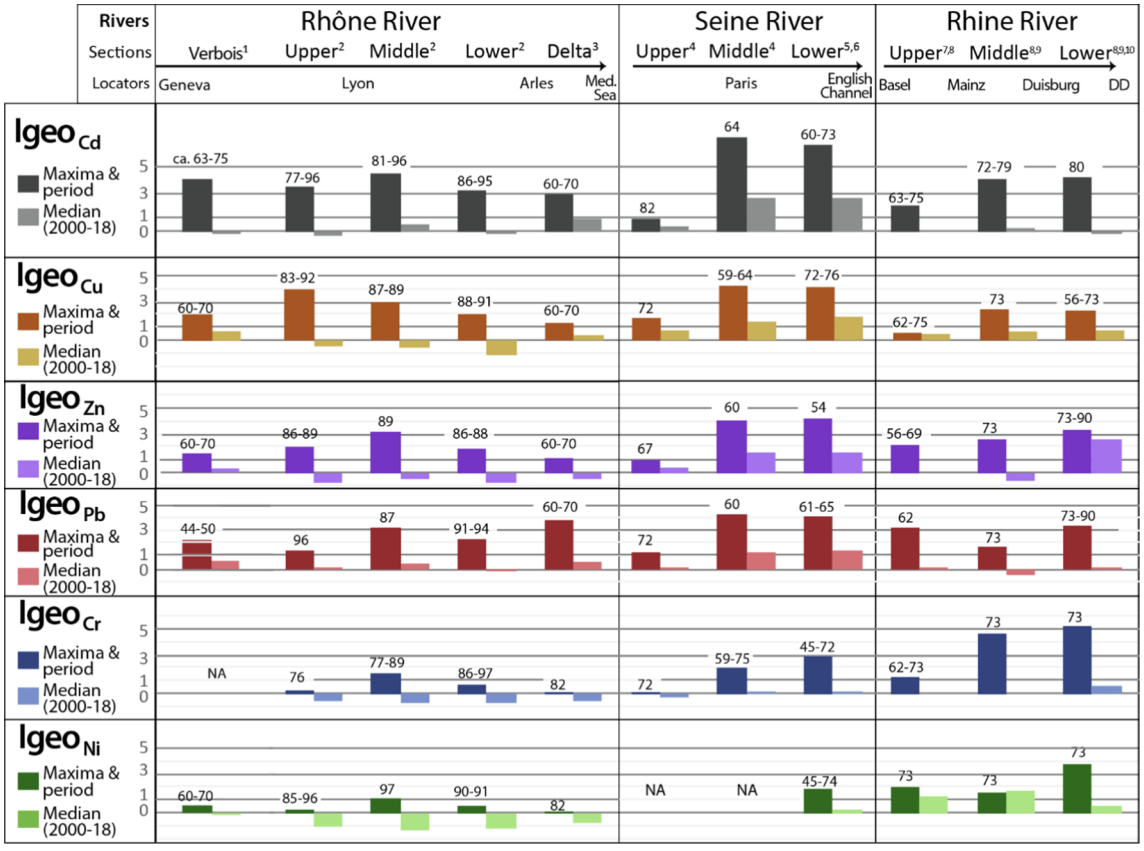

Fig. 6. Igeo trajectories along the Rhône River and in other Western European rivers (Rhine and Seine rivers). The dates above each column correspond to the period of maximal Igeo for each metal. Chronologies and Igeo were computed based on the following publications: (1) Wildi et al., 2004, 2006; (2) this article; (3) Ferrand et al., 2012; 4, Le Cloarec et al., 2011; 5, Van Metre et al., 2008; 6, Vrel, 2012; 7, Wessels et al., 1995; 8, Heise and Förstner, 2006; 9, Müller, 1986, and Middelkoop, 2000. Abridged locators: Med. Sea = Mediterranean Sea; DD = Dutch Delta of the Rhine.

and Zn ores and found in mining waste, in the Azergues basin for instance (Couturier, 2019). The increasing $Igeo_{Cd}$ before 1985 in the BRE core (GC-3) can also be linked with inputs from the Lyon Chemical Corridor and the Gier Valley, hosting smelters and steelworks (Gay, 1996). Cd-rich sediments are delivered through the Cance and the Ardèche tributaries draining the foothills of the Massif Central (granitic and metamorphic rocks) where are located the former mining districts of St-Julien-Molin-Molette (Dumoulin, 2005), L'Argentière, and Chassezac (Bailly-Maître et al., 2013; Bourg, 2013). Finally, the facilities of the Roussillon Plain were suspected to release Cd from the textile industry (nylon), and in plastic or ethyl acetate production. More recently (2000–2018), the median $Igeo_{Cd}$ is low (ca. 1) and consistent with decreasing EFs for Cd towards the Rhône delta (Ferrand et al., 2012).

The Cd trend recorded along the Rhône from the 1960s to the 1980s seems coherent with the Middle and Lower Rhine trajectories well-known to be impacted by the Main and Ruhr industries (Fig. 6; Heise and Förstner, 2006; Müller, 1986). A similar level of pollution was recorded earlier (1960s) in the Thames River sediment cores (O'Reilly Wiese et al., 1997; Vane et al., 2020). Regarding French rivers, the Cd contamination of the Rhône remains low in comparison with the Lot-Garonne system and the Seine River that were extremely polluted from 1960 to 1986 (Audry et al., 2004; Le Cloarec et al., 2011). A slow recovery of both fluvial and estuarine sediment quality is in progress in the Seine which is still moderately to heavily contaminated nowadays (Fig. 6). On the contrary, the sediments of the Rhine, and Thames rivers seem currently not very contaminated regarding the Cd general trends. The same could be observed on the Lower Garonne despite its intensive history of Cd manufacturing (Larrose et al., 2010), thanks to major remediation processes implemented in the last four decades (Pougnet et al., 2019)

4.1.3. Copper (Cu)

As reported above, a heavy Cu pollution was found in the Upper Rhône between the 1980s and 1990s, and suggested a local source ("hotspot") of pollution in the GC-2 (Figs. 1, 4, 6). The geological catchment is not enriched in Cu, but this rural area is dominated by orchards and vineyards producing the "Bugey wine" (INAO, 2012). In such a context, large amounts of copper sulphate ($CuSO_4$) used as "Bordeaux mixture" fungicide are usually leached to soil and water (Arrouays et al., 2014). In the same period, a high enrichment due to the use of $CuSO_4$ in the Champagne vineyards was also evidenced on the Aube watershed, which is a tributary of the Upper Seine (Le Cloarec et al., 2011). In addition, long-distance industrial treatment (e.g. wood impregnating process, metallurgy, building, automobile, machine equipment, pigments, surface coating) or mining releases, e.g. delivered by the Guiers and the Fier rivers, could be involved at the regional scale (Bourg, 2013; Molin, 1946).

A moderate pollution by Cu was also highlighted in the Middle Rhône Valley during the 1980s. It could be related to multiple anthropogenic releases. (1) This river section presents numerous vineyards (e.g. "Côte Rôtie", "Côteaux du Vivarais", "Côtes du Rhône") that could deliver bio-accumulable Cu (from fungicides) to the aquatic ecosystem in particular during floods (Banas et al., 2010; Mazet et al., 2005). (2) This area also experienced long-term mining due to the extraction of massive sulphide lenses in the Chessy-les-Mines district (Azergues Basin). (3) Cable production, south of Lyon (Berthet et al., 2009), and (4) nuclear power plants (St-Alban, Cruas, Tricastin) or reprocessing facilities (Marcoule) could also be sources of Cu and Zn releases for the Middle / Lower Rhône (Eyrolle et al., 2008; Winfield et al., 2006). A downstream diffusion of this pollution is supported by high Cu/Al ratios from 1960 to 1990 (GC-5 and GC-6), but also in floodplain deposits from the Middle Rhône (Vauclin et al., 2019) to its delta (Ferrand et al., 2012).

The Rhône Cu Igeo trend (1960–1990) contrasts with other Western European river trajectories, in which the Cu pollution was prevalent during the 1940s–1970s due to metal transformation in riverine facilities and industries (automobile, cables, and tube manufacturing: Callender, 2003). This hotspot period was well documented for the Rhine (Middelkoop, 2000), the Loire (Grosbois et al., 2012), Garonne (Audry et al., 2004), and Seine rivers (Le Cloarec et al., 2011). The difference between the Cu history of the Rhône and the other rivers can be explained by the regional history of human activities in each catchment.

4.1.4. Zinc (Zn)

The geo-accumulation of Zn gradually increased from the Verbois reservoir (Switzerland) to the Middle Rhône (France), where the sediments were heavily contaminated in the late 1980s (Fig. 6). Such a gradual increase along the river could be linked to urban (sewage, traffic runoff, oils, and greases of engines), mining, and industrial emissions (plating, steel, batteries, and pigments) dispersed from the Lyon conurbation. A similar hypothesis was raised to explain the contamination of the Vidy Bay in the 1960s, exposed to the release of wastewaters from Lausanne (Switzerland; cf. Gascón Díez et al., 2017; Wildi et al., 2004). Zinc, as well as copper and lead, is present in significant amounts in rural areas due to spreading and surface runoff on highways (metals derived from guard rail erosion or from the wearing of tires and brake shoes), and industrial areas (Gasperi et al., 2014; Legret and Pagotto, 2006). Their diffusion through SPM from the Rhône to its delta was highlighted by Radakovitch et al. (2008), Ollivier et al. (2011), and recently detailed by Delile et al. (In Press) during flood events.

The Rhône pattern for Zn was consistent with the sediment archives from the industrial and urban corridor of the Rhine within 1955–1990 (Fig. 6). However the maximal Zn contamination occurred earlier (1950s–1960s) on the Thames, Seine, and Loire rivers (Dhivert et al., 2015; Le Cloarec et al., 2011; Vane et al., 2020), mostly due to releases from mixing metal factories before the deindustrialisation. Finally, current median values of $Igeo_{Zn}$ are lower on the Rhône (< 0) than in other Western European rivers (Seine: 0–3) and suggest a relatively quick recovery of the sediment quality on the Rhône (ca. 8–20 years), probably due to its high sediment transport (Figs. 5 and 6).

4.1.5. Lead (Pb)

After a high geo-accumulation of Pb since the mid-1990s, our model highlighted a decreasing trend well marked in the Lower Rhône (Figs. 5 and 6). This trend differs mostly from the Seine, the Rhine, or the Loire patterns (Grosbois et al., 2012; Heise and Förstner, 2006; Meybeck et al., 2007; Wessels et al., 1995). In these rivers, geo-accumulations from upstream to downstream culminated during the 1950–1970s (Fig. 6), mainly driven by leaded gasoline combustion (Pb was used for its anti-knocking power in gasoline; Pacyna et al., 2009). The most likely explication is that the Rhône sediments recorded a mix of various industrial releases from its watershed, less influenced by atmospheric emissions of gasoline derived-Pb than other contexts (Monna et al., 1999). The latter work demonstrated that Pb derived from industrial/domestic emissions was predominant in the Geneva Lake in the 1980s–1990s, with a lower contribution from leaded gasoline. This hypothesis is suitable for the Middle Rhône Valley, where coal burning, smelters, and metal manufacturing facilities were significant in the Azergues, Gier, or Ardèche basins (Bourg, 2013). Interestingly, at the Rhône river mouth, Cossa et al. (2018) demonstrated that the industrial Pb from the Rhône highly accumulated in the Gulf of Lion canyons at the same period, and impacted the Western Mediterranean Sea (due to east–west drifting). Sediment pollution by industrial Pb was also reported in other French rivers due to coal burning, metal transformation (e.g. phosphogypsum), lead battery, cathode-ray tubes manufacturing, or glassworks, and it significantly increased after the regression of leaded gasoline (Chiffoleau et al., 2012; Dhivert et al., 2016; Gardes et al., 2020).

The second typical feature is the rapid lowering of the $Igeo_{Pb}$ at the beginning of the 2000s, especially in the Middle and Lower Rhône

(Fig. 5). In addition with the successful phasing out of Pb in gasoline (European Directive 98/70/EC of October 13, 1998), it could be imputed to the reduction of Pb in industrial processes at the nationwide scale (Pb emissions decreased by 97% in France since 1990: EEA, 2019). This short delay (from 1990 to the 2000s) suggests a rapid decrease after the regulation and a good recovery compared to POPs, such as PCBs, that decreased very slowly and reached low ecotoxic levels only 40 years after their global prohibition (Dendievel et al., 2020a).

4.2. Contribution of metal pollutants to the ecotoxicological risk mixture

The Risk Quotient mixture (RQ_{mix}) is based on metals and POPs (PCBs, BFRs, and OCPs) in order to assess the relative contribution of each pollutant to the "cocktail effect" on sediment-dwelling organisms (Fig. 7; see SI-5 for detailed RQ values and PNEC references). The RQ_{mix} distribution, inferred from the dated sediment cores along the Rhône, is analysed according to four time-periods from (a) 1965–1985, (b) 1985–1995; (c) 1995–2005, to (d) 2005–2015 (Fig. 7). Fig. 7 allows identifying a first major period (before 2005) dominated by a high risk of mixture induced by significant metals, and a second phase (since 2005) mainly driven by POPs.

Over the whole period (since 1965), RQ_{mix} generally increases according to an upstream–downstream gradient with a score regularly exceeding 70 (medium risk of ecotoxicity) in the Upper Rhône, while RQ_{mix} exceeds 100 at south, especially in the Lower Rhône (high risk at GEC). The medium mixture risk estimated in the Upper Rhône is mainly due to metals, especially Cu which is responsible for ca. 81% of the predicted cumulative risk. Indeed, Cu is known for its high impact on reproduction and biomass of benthic fauna alone, or when combined with other metals (Mahamoud Ahmed et al., 2018). The cumulated risk of mixture is especially high at MTE between 1975 and 1995 which is mainly influenced by Cu as demonstrated above (Fig. 3A; RQ_{mix} = 214–230). However, the important organic matter content of the MTE samples at this time (median = 4.4%) and the ability of Cu to complex with organic matter decreases its potential ecotoxicity, and induced a lower bioavailability than estimated by the RQ_{mix} (cf. Di Toro et al., 2005). The other elements represent less than 20% of the metal mixture in the following order (all periods): Ni (9%), Zn (4%), Pb (1%), Cd (0.4%). High ecotoxicity is estimated for Ni, although it has to be balanced because Ni is naturally present in the Rhône sediments (geogenic or agriculture erosion), and slightly released by the riverine industries (surface coating mainly). Given the influence of the Massif Central geology on the Middle Rhône sediments (right bank tributaries), the minor impact of Pb is also surprising because mining and metallurgical wastes were the most likely Pb-source of fish contamination for a long period in the upstream areas (Monna et al., 2011).

The global RQ_{mix} presents an increasing part of POPs from upstream to downstream (Fig. 7). This risk enhancement downstream of Lyon shows a change of importance and composition. Indeed, POPs signal increases from 1 to 7% (ETL and MTE, Upper Rhône) to 10–14% of the RQ_{mix} (BRE, ARS), and reaches 40–87% at GEC (Fig. 7). Such a trend is also known for other substances such as per- and poly-fluoroalkyl (Mourier et al., 2019). According to our data (SI-5), the cumulated ecotoxicity risk is mainly driven by (1) DDT metabolites (DDE and DDD), (2) Lindane isomers (HCHs), both widely used as biocides in the floodplain agriculture, and (3) PCBs that remain a major cause of concern on the Rhône (Dendievel et al., 2020a). The DDE/DDD ratio gradually increases in the river cores due to anaerobic degradation since the maximal use of DDT in the 1970s (Sabatier et al., 2014). These organic compounds frequently encountered in river and floodplain sediments worldwide can cause high toxicity and a rapid death of fishes and invertebrates, even at low concentrations (Beckvar and Lotufo, 2011).

The mixture risk along the Rhône seems high compared to other studies, although the risk estimation on river sediment rarely includes both metals and a wide range of POPs. For instance, the increase of biocide concentrations (especially carbendazim and triclosan) along the Lower Yangtze (China) leads to a high risk in water and sediments in some locations (Liu et al., 2015b). In addition, the enrichment in Cd, Cr, and Ni in the same river sediments can produce a significant risk enhancement if taken into account (Zhang et al., 2009). Along the Lower St-Louis River (Minnesota, USA), which has been documented since the 1990s, metals, PCBs, biocides (DDTs and Chlordane) and Polycyclic Aromatic Hydrocarbons (PAH) increase the mixture risk towards downstream, in particular nearby superfund sites that greatly impact the ecosystem's health (Crane and Hennes, 2007). Another example from Catalonia (Spain) highlights that the most impacted rivers are concurrently contaminated by agricultural, urban, and industrial

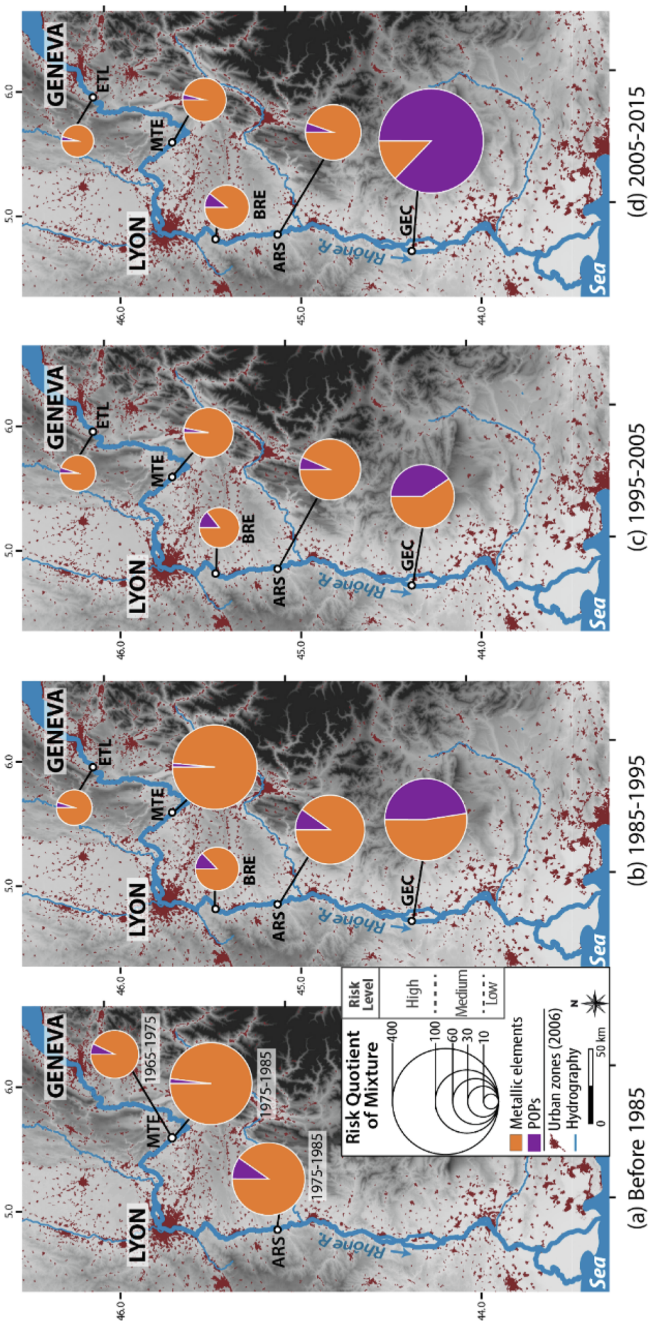

Fig. 7. Chronological map of mixture risk estimation since 1965 along the Rhône River (France). The metal data refer to this study, while POPs are from Mourier et al. (2014: PCBs) and Liber et al. (2019: PBDE 209, DDT, DDE, DDD, HBCD, HCH, HCB, and Chlordane). Data prior to 1985 for ETL, BRE and GEC are not plotted due to chronological incertitude (Mourier et al., 2014).

sources releasing organophosphate, surfactants, and metals (Ni, Cu, Cd, and Zn) (Carafa et al., 2011). The mixture risk effect could also be variable such as in the English coastal rivers (Manuel Nicolaus et al., 2015), or negligible in the Garonne Estuary (metals: Larrose et al., 2010), certainly due to sorption processes and organic matter degradation, reducing the estimation of the impact from industrial inputs in sediments, while high metal concentrations are found in fauna (Lanceleur et al., 2011). The latter cases point to the critical and current need of taking into account metals and POPs together, but also to integrate physical and socio-environmental parameters to assess the toxicity of sediments along large and heterogeneous rivers over time (Beyer et al., 2014; Kortenkamp et al., 2019).

5. Conclusion

This paper aims at reconstructing metal pollution trends along a large river by combining results from dated cores and subsurface samples acquired through research and monitoring protocols. Major issues were raised up due to the heterogeneity of the original dataset that contains limited grain-size and lithogenic information.

According to our study, both Al and Fe were relevant to normalise metal concentrations from dated cores, while only Al was grain-size correlated in background samples. This work identified some metal sources along the Rhône geographical clusters (GC): (1) the leaching of Cu from vineyards, (2) the Cd–Cu–Zn prevalence near the Hercynian Mountains (mining, slope erosion) or after urban/industrial areas, (3) the impact of industrial Pb on the Lower Rhône, and (4) the influence of geogenic Cr and Ni for the most recent deposits.

Based on local geochemical backgrounds, metal pollution trends were assessed by EFs and Igeo. They presented similar variations over time, but the lack of Al before 2010 resulted in a gap in the EF estimates. Although, the Igeo allows the use of more data to assess pollution trends. The recovery time to decrease from highly to unpolluted Igeo classes varied from 10–20 years to 30–40 years along the Rhône GC. These trends differ from other European rivers due to various geological, depositional and land-use contexts. Regarding environmental implications, we underlined the high influence of certain metals (e.g. Cu) in the risk of a cocktail of organic and inorganic contaminants. Finally, re-using European monitoring data remains challenging and calls for methodological evolutions to improve the reconstruction of pollution trajectories along large and heterogeneous rivers.

CRediT authorship contribution statement

André-Marie Dendievel: Conceptualization, Methodology, Formal analysis, Investigation, Writing - original draft. **Brice Mourier:** Conceptualization, Methodology, Writing - original draft, Supervision, Project administration, Funding acquisition. **Aymeric Dabrin:** Validation, Investigation, Writing - review & editing. **Hugo Delile:** Validation, Writing - review & editing. **Alexandra Coynel:** Methodology, Writing - review & editing. **Antoine Gosset:** Methodology, Writing - review & editing. **Yohan Liber:** Investigation, Resources. **Jean-François Berger:** Investigation, Resources, Funding acquisition. **Jean-Philippe Bedell:** Conceptualization, Resources, Supervision, Funding acquisition.

Data Availability

The dataset of the study (dated cores and samples from gauging stations) including site names, coordinates, grain-size, TOC and metal concentrations is freely available on PANGEA at https://doi.pangaea.de/10.1594/PANGAEA.914477 (Dendievel et al., 2020b). The dataset regarding the median-based geochemical background was co-submitted to *Data in Brief* (Dendievel et al., in press).

Declaration of Competing Interest

The authors declare that they have no known competing financial interests or personal relationships that could have appeared to influence the work reported in this paper.

Acknowledgments and funding

We are very grateful to Sophia Vauclin for her relevant discussion and review. We also thank Myriam Hammada and Céline Bégorre for their participation in analyses, as well as Gary Lardaux and Hervé Piégay for their help and support for the study of pre-industrial cores (CH-CO, LPP-C1, MGN-C1, EM-5) used for the geochemical background (funding: OHM “Vallée du Rhône”). Finally, we thank the two reviewers for their comments and suggestions which improved the quality of the article.

This study was conducted in the framework of the INTERPOL consortium for the comparison of the pollution trends on the main French rivers, funded by the French Office for Biodiversity (OFB). This research was supported by the Rhône Sediment Observatory (OSR), through the Plan Rhône (European Regional Development Fund), by the Rhône-Méditerranée-Corse Water Agency (RMC WA), the Rhône National Company (CNR), Electricité De France (EDF), and the regional councils from Auvergne-Rhône-Alpes, PACA and Occitanie. The metal analyses of the river cores were funded by the LabEx DRIIHM, French program “Investissements d'Avenir” (ANR-11-LABX-0010) and supported by OHM “Vallée du Rhône”.

Appendix A. Supplementary material

Supplementary data to this article can be found online at https://doi.org/10.1016/j.envint.2020.106032.

References

AFNOR, 1998. Qualité de l’eau – Dosage de huit éléments métalliques (Mn, Fe, Co, Ni, Cu, Zn, Ag, Pb) par spectrométrie d’absorption atomique dans la flamme (FD T90-112).

AFNOR, 2004. Qualité de l’eau – Dosage des éléments traces par spectrométrie d’absorption atomique en four graphite (NF EN ISO 15586).

AFNOR, 2009. Qualité de l’eau – Dosage d’éléments choisis par spectroscopie d’émission optique avec plasma induit par haute fréquence (ICP-OES) (NF EN ISO 11885).

AFNOR, 2016. Qualité de l’eau – Application de la spectrométrie de masse avec plasma à couplage inductif (ICP-MS) – Partie 2 : dosage des éléments sélectionnés y compris les isotopes d’uranium (NF EN ISO 17294-2).

Aitchison, J., 1986. The Statistical Analysis of Compositional Data. Chapman and Hall, London – New York.

Arnaud, F., Poulenard, J., Giguet-Covex, C., Wilhelm, B., Révillon, S., Jenny, J.-P., Revel, M., Enters, D., Bajard, M., Fouinat, L., Doyen, E., Simonneau, A., Pignol, C., Chapron, E., Vannière, B., Sabatier, P., 2015. Erosion under climate and human pressures: An alpine lake sediment perspective. Quat. Sci. Rev. 152, 1–18. https://doi.org/10.1016/j.quascirev.2016.09.018.

Arnaud, F., Serralongue, J., Winiarski, T., Desmet, M., 2010. An antique metallic pollution in high valley of Arve river. ArcheoSciences 34, 197–201. https://doi.org/10.4000/archeosciences.2759.

Arrouays, D., Antoni, V., Bispo, A., Brossard, M., Villanneau, E., 2014. Inventory, monitoring and state of soils in France, Europe and the world. Géosciences 18, 16–23.

Audry, S., Schäfer, J., Blanc, G., Jouanneau, J.-M., 2004. Fifty-year sedimentary record of heavy metal pollution (Cd, Zn, Cu, Pb) in the Lot River reservoirs (France). Environ. Pollut. 132, 413–426. https://doi.org/10.1016/j.envpol.2004.05.025.

Backhaus, T., Faust, M., 2012. Predictive environmental risk assessment of chemical mixtures: a conceptual framework. Environ. Sci. Technol. 46, 2564–2573. https://doi.org/10.1021/es2034125.

Bailly-Maître, M.-C., 2010. Silver of the Middle Ages: techniques for furthering seigneurial ambitions. Mélanges de l’École française de Rome 122, 451–469. https://doi.org/10.4000/mefrm.688.

Bailly-Maître, M.-C., Minvielle Larousse, N., Kammenthaler, E., Gonon Guergana Guionova, T., 2013. L’exploitation minière dans la vallée du Chassezac (Ardèche): le plomb, l’argent et le cuivre au Moyen Âge (XIe-XIIIe siècles). Archéologie Médiévale 43, 11–40.

Banas, D., Marin, B., Skraber, S., Chopin, E.I.B., Zanella, A., 2010. Copper mobilization affected by weather conditions in a stormwater detention system receiving runoff waters from vineyard soils (Champagne, France). Environ. Pollut. 158, 476–482. https://doi.org/10.1016/j.envpol.2009.08.034.

Beckvar, N., Lotufo, G.R., 2011. DDT and OtherOrganohalogen Pesticidesin Aquatic Organisms. In: Beyer, W.N., Meador, J.P. (Eds.), Environmental Contaminants in

Biota: Interpreting Tissue Concentrations. CRC Press, Boca Raton (Florida, USA), pp. 47–101.
Berthet, F., Cigolotti, A., Wasserstrom, S., 2009. Atlas de l'aventure industrielle de l'agglomération lyonnaise (XIXe - XXIe siècle). Agence d'urbanisme pour le développement de l'agglomération lyonnaise, Lyon.
Beyer, J., Petersen, K., Song, Y., Ruus, A., Grung, M., Bakke, T., Tollefsen, K.E., 2014. Environmental risk assessment of combined effects in aquatic ecotoxicology: A discussion paper. Mar. Environ. Res. 96, 81–91. https://doi.org/10.1016/j.marenvres.2013.10.008.
Blott, S.J., Pye, K., 2012. Particle size scales and classification of sediment types based on particle size distributions: Review and recommended procedures. Sedimentology 59, 2071–2096.
Bourg, C., 2013. Métaux et métalloïdes. In: Noars, F. (Ed.), Micropolluants Dans Les Sédiments de La Région Rhône-Alpes. Données Cours d'eau et Plans d'eau 2006–2011. DREAL Rhône-Alpes, Lyon, pp. 14–35.
Bravard, J.-P., 2010. Discontinuities in braided patterns: The River Rhône from Geneva to the Camargue delta before river training. Geomorphology 117, 219–233. https://doi.org/10.1016/j.geomorph.2009.01.020.
Bravard, J.-P., Bethemont, J., 2018. Pour saluer le Rhône. Libel, Lyon.
Bravard, J.-P., Provansal, M., Arnaud-Fassetta, G., Chabbert, S., Gaydou, P., Dufour, S., Richard, F., Valleteau, S., Melun, G., Passy, P., 2008. A Palaeo-enviromnetal atlas of the Rhône River alluvial plain from the Switzerland border to the Mediterranean Sea. Cahiers de Paléoenvironnement, collection EDYTEM 6, 101–116.
Brenner, R.C., Magar, V.S., Ickes, J.A., Foote, E.A., Abbott, J.E., Bingler, L.S., Crecelius, E.A., 2004. Long-term recovery of PCB-contaminated surface sediments at the Sangamo-Weston/Twelvemile Creek/Lake Hartwell Superfund Site. Environ. Sci. Technol. 38, 2328–2337. https://doi.org/10.1021/es030650d.
Callender, E., 2003. 9.03 – Heavy metals in the environment—historical trends. In: Holland, H.D., Turekian, K.K. (Eds.), Treatise on Geochemistry. Pergamon, Oxford, pp. 67–105. https://doi.org/10.1016/B0-08-043751-6/09161-1.
Carafa, R., Faggiano, L., Real, M., Munné, A., Ginebreda, A., Guasch, H., Flo, M., Tirapu, L., der Ohe, P.C. von, 2011. Water toxicity assessment and spatial pollution patterns identification in a Mediterranean River Basin District. Tools for water management and risk analysis. Sci. Total Environ. 409, 4269–4279. https://doi.org/10.1016/j.scitotenv.2011.06.053.
Cauuet, B., 2013. Les ressources métallifères du Massif central à l'âge du Fer. In: Verger, S., Pernet, L. (Eds.), Une Odyssée Gauloise. Editions Errance, Arles, pp. 86–93.
Chamley, H., 2003. Chemical Contamination of Earth's Surface Formations. In: Chamley, H. (Ed.), Geosciences, Environment and Man. Elsevier, Amsterdam, pp. 404–449.
Chiffoleau, J.-F., Sonke, J.E., Auger, D., Bretaudeau, J., Joguet, T., Larrieu, M., Laffont, L., Prunier, J., Rozuel, E., Zouiten, C., 2012. ISOMET. Etude de la signature isotopique des métaux dans l'estuaire de la Seine. Une information essentielle pour le traçage et la discrimination des sources et processus. Rapport Seine Aval 4, 1–45.
Cossa, D., Fanget, A.-S., Chiffoleau, J.-F., Bassetti, M.-A., Buscail, R., Dennielou, B., Briggs, K., Arnaud, M., Guédron, S., Berné, S., 2018. Chronology and sources of trace elements accumulation in the Rhône pro-delta sediments (Northwestern Mediterranean) during the last 400years. Prog. Oceanogr. 163, 161–171. https://doi.org/10.1016/j.pocean.2017.01.008.
Couturier, J.-P., 2019. Métallogénie et histoire minière du Massif central, in: Histoire de la découverte du Massif Central Français. Mémoire 8. Société d'Histoire Naturelle d'Auvergne, Clermont-Ferrand, pp. 174–187.
Covaci, A., Gheorghe, A., Voorspoels, S., Maervoet, J., Steen Redeker, E., Blust, R., Schepens, P., 2005. Polybrominated diphenyl ethers, polychlorinated biphenyls and organochlorine pesticides in sediment cores from the Western Scheldt river (Belgium): analytical aspects and depth profiles. Environ. Int. 31, 367–375. https://doi.org/10.1016/j.envint.2004.08.009.
Crane, J.L., Hennes, S., 2007. Guidance for the use and application of sediment quality targets for the protection of sediment-dwelling organisms in Minnesota. Minnesota Pollution Control Agency, St Paul (MN, USA).
De Vos, W., Demetriades, A., Marsina, K., Ottesen, R.T., Reeder, S., Pirc, S., Salminen, R., Tarvainen, T., 2006. Comparison of elements in all sample media, general comments and conclusions. In: De Vos, W., Tarvainen, T. (Eds.), Geochemical Atlas of Europe. Part 2 – Interpretation of Geochemical Maps, Additional Tables, Figures, Maps, and Related Publications. Geological Survey of Finland, Otamedia Oy, Espoo, pp. 45–432.
Delile, H., Masson, M., Miège, C., Le Coz, J., Poulier, G., Le Bescond, C., Radakovitch, O., Coquery, M., 2020. Hydro-climatic drivers of land-based organic and inorganic particulate micropollutant fluxes: The regime of the largest river water inflow of the Mediterranean Sea. Water Res. 116067. https://doi.org/10.1016/j.watres.2020.116067.
Dendievel, A.-M., Mourier, B., Coynel, A., Evrard, O., Labadie, P., Ayrault, S., Debret, M., Koltalo, F., Copard, Y., Faivre, Q., Gardes, T., Vauclin, S., Budzinski, H., Grosbois, C., Winiarski, T., Desmet, M., 2020a. Spatio-temporal assessment of the PCB sediment contamination in four major French river corridors (1945–2018). Earth Syst. Sci. Data. https://doi.org/10.5194/essd-2019-167.
Dendievel, A.-M., Bedell, J.-P., Cayambo, S., Hamada, M., Liber, Y., Thomas, M., Mourier, B., 2020b. Database of metal concentrations measured in sediment cores (1965–2011) and bed and flood sediments (1987–2018) along the Rhône River. PANGAEA, https://doi.pangaea.de/10.1594/PANGAEA.914477.
Dendievel, A.-M., Mourier, B., Barra, A., Bégorre, C., Dabrin, A., Hamada, M., Lardaux, G., Berger, J.-F. (in press). Dataset of natural metal background levels inferred from pre-industrial palaeochannels sediment cores along the Rhône River (France). Data In Brief. https://doi.org/10.1016/j.dib.2020.106256.
Deycard, V.N., Schäfer, J., Blanc, G., Coynel, A., Petit, J.C.J., Lanceleur, L., Dutruch, L., Bossy, C., Ventura, A., 2014. Contributions and potential impacts of seven priority substances (As, Cd, Cu, Cr, Ni, Pb, and Zn) to a major European Estuary (Gironde Estuary, France) from urban wastewater. Mar. Chem. Estuarine Biogeochem. 167, 123–134. https://doi.org/10.1016/j.marchem.2014.05.005.
Dhivert, E., Grosbois, C., Courtin-Nomade, A., Bourrain, X., Desmet, M., 2016. Dynamics of metallic contaminants at a basin scale — Spatial and temporal reconstruction from four sediment cores (Loire fluvial system, France). Sci. Total Environ. 541, 1504–1515. https://doi.org/10.1016/j.scitotenv.2015.09.146.
Dhivert, E., Grosbois, C., Rodrigues, S., Desmet, M., 2015. Influence of fluvial environments on sediment archiving processes and temporal pollutant dynamics (Upper Loire River, France). Sci. Total Environ. 505, 121–136. https://doi.org/10.1016/j.scitotenv.2014.09.082.
Di Toro, D.M., McGrath, J.A., Hansen, D.J., Berry, W.J., Paquin, P.R., Mathew, R., Wu, K.B., Santore, R.C., 2005. Predicting sediment metal toxicity using a sediment biotic ligand model: methodology and initial application. Environ. Toxicol. Chem. 24, 2410–2427. https://doi.org/10.1897/04-413R.1.
Doong, R., Lee, S., Lee, C., Sun, Y., Wu, S., 2008. Characterization and composition of heavy metals and persistent organic pollutants in water and estuarine sediments from Gao-ping River, Taiwan. Mar. Pollut. Bull. 57, 846–857. https://doi.org/10.1016/j.marpolbul.2007.12.015.
Dumoulin, F., 2005. Les mines métallifères du département de la Loire. Bilan de sept années de recherches. Revue Archéologique du Centre de la France, 271–276.
ECB, 2001. European Union Risk Assessment Report. CAS No.: 32534-81-9. EINECS No.: 251-084-2. Diphenyl ether, pentabromo deriv. European Communities, Luxembourg.
ECB, 2003. Technical Guidance Document (TGD) for risk assessment in support of Commission Directive 93/67/EEC on Risk Assessment for new notified substances Commission Regulation (EC) No 1488/94 on Risk Assessment for existing substances Directive 98/8/EC of the European Parliament and of the Council concerning the placing of biocidal products on the market. European communities, Ispra (Italy).
EEA, 2019. Heavy Metal Emissions. European Environment Agency, Copenhagen.
Eyrolle, F., Claval, D., Gontier, G., Antonelli, C., 2008. Radioactivity levels in major French rivers: summary of monitoring chronicles acquired over the past thirty years and current status. J. Environ. Monit. 10, 800–811. https://doi.org/10.1039/B805752B.
Ferrand, E., Eyrolle, F., Radakovitch, O., Provansal, M., Dufour, S., Vella, C., Raccasi, G., Gurriaran, R., 2012. Historical levels of heavy metals and artificial radionuclides reconstructed from overbank sediment records in lower Rhône River (South-East France). Geochim. Cosmochim. Acta 82, 163–182. https://doi.org/10.1016/j.gca.2011.11.023.
Förstner, U., Salomons, W., 1980. Trace metal analysis on polluted sediments. Environ. Technol. Lett. 1, 494–505. https://doi.org/10.1080/09593338009384006.
Fung, Y.S., Lo, C.K., 1997. Determination of heavy metal profiles in dated sediment cores from Sai Kung Bay, Hong Kong. Environ. Int. 23, 317–335. https://doi.org/10.1016/S0160-4120(97)00034-2.
Gardes, T., Debret, M., Copard, Y., Coynel, A., Deloffre, J., Fournier, M., Revillon, S., Nizou, J., Develle, A.-L., Sabatier, P., Marcotte, S., Patault, E., Faivre, Q., Portet-Koltalo, F., 2020. Flux estimation, temporal trends and source determination of trace metal contamination in a major tributary of the Seine estuary, France. Sci. Total Environ. 724, 138249. https://doi.org/10.1016/j.scitotenv.2020.138249.
Gascón Díez, E., Corella, J.P., Adatte, T., Thevenon, F., Loizeau, J.-L., 2017. High-resolution reconstruction of the 20th century history of trace metals, major elements, and organic matter in sediments in a contaminated area of Lake Geneva, Switzerland. Appl. Geochem. 78, 1–11. https://doi.org/10.1016/j.apgeochem.2016.12.007.
Gasperi, J., Sebastian, C., Ruban, V., Delamain, M., Percot, S., Wiest, L., Mirande, C., Caupos, E., Demare, D., Kessoo, M.D.K., Saad, M., Schwartz, J.J., Dubois, P., Fratta, C., Wolff, H., Moilleron, R., Chebbo, G., Cren, C., Millet, M., Barraud, S., Gromaire, M.C., 2014. Micropollutants in urban stormwater: occurrence, concentrations, and atmospheric contributions for a wide range of contaminants in three French catchments. Environ. Sci. Pollut. Res. 21, 5267–5281. https://doi.org/10.1007/s11356-013-2396-0.
Garrett, R.G., 2018. Package 'rgr'. Appl. Geochem. EDA. Version 1.1.15.
Gay, G., 1996. Mines, forges et usines dans la vallée du Gier (Loire): le patrimoine industriel comme palimpseste social. Le Monde alpin et rhodanien. Revue régionale d'ethnologie 24, 215–229. https://doi.org/10.3406/mar.1996.1609.
Gil-Díaz, T., Schäfer, J., Dutruch, L., Bossy, C., Pougnet, F., Abdou, M., Lerat-Hardy, A., Pereto, C., Derriennic, H., Briant, N., Sireau, T., Knoery, J., Blanc, G., 2019. Tellurium behaviour in a major European fluvial–estuarine system (Gironde, France): fluxes, solid/liquid partitioning and bioaccumulation in wild oysters. Environ. Chem. 16, 229–242. https://doi.org/10.1071/EN18226.
Gosset, A., Polomé, P., Perrodin, Y., 2020. Ecotoxicological risk assessment of micropollutants from treated urban wastewater effluents for watercourses at a territorial scale: Application and comparison of two approaches. Int. J. Hyg. Environ. Health 224, 113437. https://doi.org/10.1016/j.ijheh.2019.113437.
Grygar, T.M., Elznicová, J., Kiss, T., Smith, H.G., 2016. Using sedimentary archives to reconstruct pollution history and sediment provenance: The Ohře River, Czech Republic. CATENA 144, 109–129. https://doi.org/10.1016/j.catena.2016.05.004.
Grosbois, C., Meybeck, M., Horowitz, A., Ficht, A., 2006. The spatial and temporal trends of Cd, Cu, Hg, Pb and Zn in Seine River floodplain deposits (1994–2000). Sci. Total Environ. 356, 22–37. https://doi.org/10.1016/j.scitotenv.2005.01.049.
Grosbois, C., Meybeck, M., Lestel, L., Lefèvre, I., Moatar, F., 2012. Severe and contrasted polymetallic contamination patterns (1900–2009) in the Loire River sediments (France). Sci. Total Environ. 435–436, 290–305. https://doi.org/10.1016/j.scitotenv.2012.06.056.
Halitim-Dubois, N., 2019. Industries en Héritage. Auvergne-Rhône-Alpes. Lieux Dits Editions, Lyon.
Heise, S., Förstner, U., 2006. Risks from historical contaminated sediments in the Rhine Basin. Water Air Soil Pollut. Focus 6, 625–636. https://doi.org/10.1007/s11267-006-9047-0.
Helsel, D.R., 2012. Statistics for Censored Environmental Data using Minitab and R.

Wiley, Hoboken (NJ, USA).
INAO, 2012. AOC Bugey. AOC Bugey suivie d'une dénomination. Vineyard map, https://www.inao.gouv.fr/var/inao_site/storage/repository/editeur/files/pdf/Cartes/AOC_Bugeydenominations_A_201201.pdf.
JORF, 2006. Arrêté du 9 août 2006 relatif aux niveaux à prendre en compte lors d'une analyse de rejets dans les eaux de surface ou de sédiments marins, estuariens ou extraits de cours d'eau ou canaux relevant respectivement des rubriques 2.2.3.0, 4.1.3.0 et 3.2.1.0 de la nomenclature annexée au décret n° 93–743 du 29 mars 1993. Journal Officiel de la République Française 222, 14082.
Kortenkamp, A., Faust, M., Backhaus, T., Altenburger, R., Scholze, M., Müller, C., Ermler, S., Posthuma, L., Brack, W., 2019. Mixture risks threaten water quality: the European Collaborative Project SOLUTIONS recommends changes to the WFD and better co-ordination across all pieces of European chemicals legislation to improve protection from exposure of the aquatic environment to multiple pollutants. Environ. Sci. Eur. 31, 69. https://doi.org/10.1186/s12302-019-0245-6.
Lafargue, E., Marquis, F., Pillot, D., 1998. Rock-Eval 6 applications in hydrocarbon exploration, production, and soil contamination studies. Rev. Inst. Fr. Pét. 53, 421–437. https://doi.org/10.2516/ogst:1998036.
Lanceleur, L., Schäfer, J., Chiffoleau, J.-F., Blanc, G., Auger, D., Renault, S., Baudrimont, M., Audry, S., 2011. Long-term records of cadmium and silver contamination in sediments and oysters from the Gironde fluvial–estuarine continuum – Evidence of changing silver sources. Chemosphere 85, 1299–1305. https://doi.org/10.1016/j.chemosphere.2011.07.036.
Larrose, A., Coynel, A., Schäfer, J., Blanc, G., Massé, L., Maneux, E., 2010. Assessing the current state of the Gironde Estuary by mapping priority contaminant distribution and risk potential in surface sediment. Appl. Geochem. 25, 1912–1923. https://doi.org/10.1016/j.apgeochem.2010.10.007.
Le Cloarec, M.-F., Bonte, P.H., Lestel, L., Lefèvre, I., Ayrault, S., 2011. Sedimentary record of metal contamination in the Seine River during the last century. Phys. Chem. Earth. 36, 515–529. https://doi.org/10.1016/j.pce.2009.02.003.
Legret, M., Pagotto, C., 2006. Heavy metal deposition and soil pollution along two major rural highways. Environ. Technol. 27, 247–254. https://doi.org/10.1080/09593332708618641.
Liber, Y., Mourier, B., Marchand, P., Bichon, E., Perrodin, Y., Bedell, J.-P., 2019. Past and recent state of sediment contamination by persistent organic pollutants (POPs) in the Rhône River: Overview of ecotoxicological implications. Sci. Total Environ. 646, 1037–1046. https://doi.org/10.1016/j.scitotenv.2018.07.340.
Liu, W.-R., Zhao, J.-L., Liu, Y.-S., Chen, Z.-F., Yang, Y.-Y., Zhang, Q.-Q., Ying, G.-G., 2015a. Biocides in the Yangtze River of China: Spatiotemporal distribution, mass load and risk assessment. Environ. Pollut. 200, 53–63. https://doi.org/10.1016/j.envpol.2015.02.013.
Liu, R., Tan, R., Li, B., Song, Y., Zeng, P., Li, Z., 2015b. Overview of POPs and heavy metals in Liao River Basin. Environ. Earth Sci. 73, 5007–5017. https://doi.org/10.1007/s12665-015-4317-7.
MacDonald, D.D., Dipinto, L.M., Field, J., Ingersoll, C.G., Lvong, E.R., Swartz, R.C., 2000a. Development and evaluation of consensus-based sediment effect concentrations for polychlorinated biphenyls. Environ. Toxicol. Chem. 19, 1403–1413. https://doi.org/10.1002/etc.5620190524.
MacDonald, D.D., Ingersoll, C.G., Berger, T.A., 2000b. Development and evaluation of consensus-based sediment quality guidelines for freshwater ecosystems. Arch. Environ. Contam. Toxicol. 39, 20–31. https://doi.org/10.1007/s002440010075.
Mahamoud Ahmed, A., Lyautey, E., Bonnineau, C., Dabrin, A., Pesce, S., 2018. Environmental concentrations of copper, alone or in mixture with arsenic, can impact river sediment microbial community structure and functions. Front. Microbiol. 9. https://doi.org/10.3389/fmicb.2018.01852.
Manuel Nicolaus, E.E., Law, R.J., Wright, S.R., Lyons, B.P., 2015. Spatial and temporal analysis of the risks posed by polycyclic aromatic hydrocarbon, polychlorinated biphenyl and metal contaminants in sediments in UK estuaries and coastal waters. Mar. Pollut. Bull. 95, 469–479. https://doi.org/10.1016/j.marpolbul.2015.03.012.
Mazet, A., Keck, G., Berny, P., 2005. Concentrations of PCBs, organochlorine pesticides and heavy metals (lead, cadmium, and copper) in fish from the Drôme river: Potential effects on otters (*Lutra lutra*). Chemosphere 61, 810–816. https://doi.org/10.1016/j.chemosphere.2005.04.056.
Meybeck, M., 2013. Heavy metal contamination in rivers across the globe: an indicator of complex interactions between societies and catchments. In: Arheimer, B. (Ed.), Understanding Freshwater Quality Problems in a Changing World. IAHS Press, Wallingford, pp. 3–16.
Meybeck, M., Lestel, L., Bonté, P., Moilleron, R., Colin, J.L., Rousselot, O., Hervé, D., de Pontevès, C., Grosbois, C., Thévenot, D., 2007. Historical perspective of heavy metals contamination (Cd, Cr, Cu, Hg, Pb, Zn) in the Seine River basin (France) following a DPSIR approach (1950–2005). Sci. Total Environ. 375, 204–231. https://doi.org/10.1016/j.scitotenv.2006.12.017.
Meybeck, M., Lestel, L., Carré, C., Bouleau, G., Garnier, J., Mouchel, J.M., 2018. Trajectories of river chemical quality issues over the Longue Durée: the Seine River (1900S–2010). Environ. Sci. Pollut. Res. 25, 23468–23484. https://doi.org/10.1007/s11356-016-7124-0.
Middelkoop, H., 2000. Heavy-metal pollution of the river Rhine and Meuse floodplains in the Netherlands. Netherlands J. Geosci. 78 (4), 411–427. https://doi.org/10.1017/S0016774600021910.
Molin, J., 1946. Une curieuse concentration d'industries à l'écart des grandes villes : Le bassin moyen des Guiers. Revue de Géographie Alpine 34, 447–468. https://doi.org/10.3406/rga.1946.5225.
Monna, F., Camizuli, E., Revelli, P., Biville, C., Thomas, C., Losno, R., Scheifler, R., Bruguier, O., Baron, S., Chateau, C., Ploquin, A., Alibert, P., 2011. Wild Brown Trout Affected by Historical Mining in the Cevennes National Park, France. Environ. Sci. Technol. 45, 6823–6830.
Monna, F., Dominik, J., Loizeau, J.-L., Pardos, M., Arpagaus, P., 1999. Origin and Evolution of Pb in Sediments of Lake Geneva (Switzerland–France). Establishing a Stable Pb Record. Environ. Sci. Technol. 33, 2850–2857.
Moore, J.N., Langner, H.W., 2012. Can a river heal itself? Natural attenuation of metal contamination in river sediment. Environ. Sci. Technol. 46, 2616–2623. https://doi.org/10.1021/es203810j.
Mourier, B., Desmet, M., Van Metre, P.C., Mahler, B.J., Perrodin, Y., Roux, G., Bedell, J.-P., Lefèvre, I., Babut, M., 2014. Historical records, sources, and spatial trends of PCBs along the Rhône River (France). Sci. Total Environ. 476–477, 568–576. https://doi.org/10.1016/j.scitotenv.2014.01.026.
Mourier, B., Labadie, P., Desmet, M., Grosbois, C., Raux, J., Debret, M., Copard, Y., Pardon, P., Budzinski, H., Babut, M., 2019. Combined spatial and retrospective analysis of fluoroalkyl chemicals in fluvial sediments reveal changes in levels and patterns over the last 40 years. Environ. Pollut. 253, 1117–1125. https://doi.org/10.1016/j.envpol.2019.07.079.
Müller, G., 1979. Schwermetalle in den Sedimenten des Rheins-Veränderungen seit 1971. Umschau in Wissenschaft und Technik 79, 778–783.
Müller, G., 1986. Schadstoffe in Sedimenten - Sedimente als Schadstoffe. Umweltgeologie-Band 79, 107–126.
Norwood, W.P., Borgmann, U., Dixon, D.G., Wallace, A., 2003. Effects of metal mixtures on aquatic biota: a review of observations and methods. Hum. Ecol. Risk Assess.: Int. J. 9, 795–811. https://doi.org/10.1080/713610010.
Olivier, J.-M., Carrel, G., Lamouroux, N., Dole-Olivier, M.-J., Malard, F., Bravard, J.-P., Amoros, C., 2009. The Rhône River Basin. In: Tockner, K., Robinson, C.T., Uehlinger, U. (Eds.), Rivers of Europe. Academic Press, London, pp. 247–295.
Ollivier, P., Radakovitch, O., Hamelin, B., 2011. Major and trace element partition and fluxes in the Rhône River. Chem. Geol. 285, 15–31. https://doi.org/10.1016/j.chemgeo.2011.02.011.
O'Reilly Wiese, S.B., MacLeod, C.L., Lester, J.N., 1997. A recent history of metal accumulation in the sediments of the Thames Estuary, United Kingdom. Estuaries 20, 483. https://doi.org/10.2307/1352608.
Pacyna, J.M., Pacyna, E.G., Aas, W., 2009. Changes of emissions and atmospheric deposition of mercury, lead, and cadmium. Atmos. Environ. – Fifty Years of Endeavour 43, 117–127. https://doi.org/10.1016/j.atmosenv.2008.09.066.
Pelletier, M., Blais, S., 2018. Sediment quality in the St. Lawrence River in the Quebec sector in 2012 and its evolution since 1989. Her Majesty the Queen in Right of Canada, represented by the Minister of Environment and Climate Change & Government of Quebec.
Perrodin, Y., Donguy, G., Bazin, C., Volatier, L., Durrieu, C., Bony, S., Devaux, A., Abdelghafour, M., Moretto, R., 2012. Ecotoxicological risk assessment linked to infilling quarries with treated dredged seaport sediments. Sci. Total Environ. 431, 375–384. https://doi.org/10.1016/j.scitotenv.2012.05.069.
Pinglot, J.F., Pourchet, M., 1995. Radioactivity measurements applied to glaciers and lake sediments. Sci. Total Environ., Environ. Radiochem. Anal. 173–174, 211–223. https://doi.org/10.1016/0048-9697(95)04779-4.
Pougnet, F., Blanc, G., Mulamba-Guilhemat, E., Coynel, A., Gil-Diaz, T., Bossy, C., Strady, E., Schäfer, J., 2019. New computation for a better estimation of the annual dissolved metal net fluxes. The case of the cadmium in the Gironde estuary. Hydroécol. Appl. https://doi.org/10.1051/hydro/2019002.
Poulier, G., Launay, M., Le Bescond, C., Thollet, F., Coquery, M., Le Coz, J., 2019. Combining flux monitoring and data reconstruction to establish annual budgets of suspended particulate matter, mercury and PCB in the Rhône River from Lake Geneva to the Mediterranean Sea. Sci. Total Environ. 658, 457–473. https://doi.org/10.1016/j.scitotenv.2018.12.075.
Priadi, C., Bourgeault, A., Ayrault, S., Gourlay-Francé, C., Tusseau-Vuillemin, M.-H., Bonté, P., Mouchel, J.-M., 2011. Spatio-temporal variability of solid, total dissolved and labile metal: passive vs. discrete sampling evaluation in river metal monitoring. J. Environ. Monit. 13, 1470–1479. https://doi.org/10.1039/C0EM00713G.
Provansal, M., Berger, J.-F., Bravard, J.-P., Salvador, P.-G., Arnaud-Fassetta, G., Bruneton, H., Vérot-Bourrély, A., 1999. Le régime du Rhône dans l'Antiquité et au Haut Moyen Age. Gallia 56, 13–32. https://doi.org/10.3406/galia.1999.3241.
R Core Team, 2018. R: A language and environment for statistical computing. Version 3.5.2 Eggshell Igloo. R Foundation for Statistical Computing, Vienna (Austria).
Radakovitch, O., Roussiez, V., Ollivier, P., Ludwig, W., Grenz, C., Probst, J.-L., 2008. Input of particulate heavy metals from rivers and associated sedimentary deposits on the Gulf of Lion continental shelf. Estuar. Coast. Shelf Sci. 77, 285–295. https://doi.org/10.1016/j.ecss.2007.09.028.
Reimann, C., de Caritat, P., 2000. Intrinsic flaws of element enrichment factors (EFs) in environmental geochemistry. Environ. Sci. Technol. 34, 5084–5091. https://doi.org/10.1021/es001339o.
Reimann, C., Filzmoser, P., Garrett, R.G., 2005. Background and threshold: critical comparison of methods of determination. Sci. Total Environ. 346, 1–16. https://doi.org/10.1016/j.scitotenv.2004.11.023.
Reimann, C., Garrett, R.G., 2005. Geochemical background—concept and reality. Sci. Total Environ. 350, 12–27. https://doi.org/10.1016/j.scitotenv.2005.01.047.
Reimer, P., Bard, E., Bayliss, A., Beck, J.W., Blackwell, P., Bronk Ramsey, C., Buck, C., Cheng, H., Edwards, R.L., Friedrich, M., Grootes, P., Guilderson, T., Haflidason, H., Hajdas, I., Hatté, C., Heaton, T., Hoffmann, D., Hogg, A., Hughen, K., Kaiser, K.F., Kromer, B., Manning, S., Niu, M., Reimer, R., Richards, D., Scott, E.M., Southon, J., Staff, R., Turney, C., van der Plicht, J., 2013. Intcal13 and Marine13 radiocarbon age calibration curves 0–50,000 years cal BP. Radiocarbon 55, 1869–1887. https://doi.org/10.2458/azu_js_rc.55.16947.
Reuther, R., 2009. Lake and river sediment monitoring. In: Inyang, H.I. and Daniels J.L. (Eds.), Encyclopedia of Life Support Systems. Environmental Monitoring – Volume II. Eolss, Oxford, pp. 120–147.
Rudnick, R.L., Gao, S., 2014. Composition of the Continental Crust. In: Holland, H.D.,

Turekian, K.K. (Eds.), Treatise on Geochemistry, Second edition, Volume 4. Elsevier, Amsterdam, pp. 1–51. https://doi.org/10.1016/B978-0-08-095975-7.00301-6.
Sabatier, P., Poulenard, J., Fanget, B., Reyss, J.-L., Develle, A.-L., Wilhelm, B., Ployon, E., Pignol, C., Naffrechoux, E., Dorioz, J.-M., Montuelle, B., Arnaud, F., 2014. Long-term relationships among pesticide applications, mobility, and soil erosion in a vineyard watershed. PNAS 111, 15647–15652. https://doi.org/10.1073/pnas.1411512111.
Salvador, P.-G., Berger, J.-F., 2014. The evolution of the Rhone River in the Basses Terres basin during the Holocene (Alpine foothills, France). Geomorphology 204, 71–85. https://doi.org/10.1016/j.geomorph.2013.07.030.
Salvador, P.-G., Berger, J.-F., Fontugne, M., Gauthier, Emilie, 2005. Sedimentary fillings study of the Holocene Rhône river palaeomeanders on the Basses Terres floodplain (Isère, Ain, France). Quaternaire 16, 315–327. https://doi.org/10.4000/quaternaire.517.
Santschi, P.H., Presley, B.J., Wade, T.L., Garcia-Romero, B., Baskaran, M., 2001. Historical contamination of PAHs, PCBs, DDTs, and heavy metals in Mississippi River Delta, Galveston Bay and Tampa Bay sediment cores. Mar. Environ. Res. 52, 51–79. https://doi.org/10.1016/S0141-1136(00)00260-9.
Sauquet, E., Gottschalk, L., Krasovskaia, I., 2008. Estimating mean monthly runoff at ungauged locations: an application to France. Hydrol. Res. 39, 403–423. https://doi.org/10.2166/nh.2008.331.
Smith, E.P., Robinson, T., Field, L.J., Norton, S.B., 2003. Predicting sediment toxicity using logistic regression: a concentration-addition approach. Environ. Toxicol. Chem. 22, 565–575.
Sun, X., Fan, D., Liu, M., Tian, Y., Pang, Y., Liao, H., 2018. Source identification, geochemical normalization and influence factors of heavy metals in Yangtze River Estuary sediment. Environ. Pollut. 241, 938–949. https://doi.org/10.1016/j.envpol.2018.05.050.
Tang, J., Chai, L., Li, H., Yang, Z., Yang, W., 2018. A 10-year statistical analysis of heavy metals in river and sediment in hengyang segment, Xiangjiang River Basin, China. Sustainability 10, 1057. https://doi.org/10.3390/su10041057.
Tena, A., Piégay, H., Seignemartin, G., Barra, A., Berger, J.F., Mourier, B., Winiarski, T., 2020. Cumulative effects of channel correction and regulation on floodplain terrestrialisation patterns and connectivity. Geomorphology 354, 107034. https://doi.org/10.1016/j.geomorph.2020.107034.
Thévenot, D., Meybeck, M., Chestérikoff, A., Chevreuil, M., 1998. Métaux: sources multiples et accumulation. In: Meybeck, M., De Marsily, G., Fustec, E. (Eds.), La Seine en son Bassin. Elsevier, Paris, Amsterdam, Lausanne, pp. 391–437.
Thévenot, D., Moilleron, R., Lestel, L., Gromaire, M.-C., Rocher, V., Cambier, P., Bonté, P., Colin, J.-L., de Pontevès, C., Meybeck, M., 2007. Critical budget of metal sources and pathways in the Seine River basin (1994–2003) for Cd, Cr, Cu, Hg, Ni, Pb and Zn. Sci. Total Environ. 375, 180–203. https://doi.org/10.1016/j.scitotenv.2006.12.008.
Thomas, R., Meybeck, M., 1996. Chapter 4 – The use of particulate material. In: Chapman, D., UNESCO/WHO/UNEP (Eds.), Water Quality Assessments: A Guide to the Use of Biota, Sediments and Water in Environmental Monitoring, second edition, E & FN Spon, London, 626 p.
Thollet, F., Le Bescond, C., Lagouy, M., Gruat, A., Grisot, G., Le Coz, J., Coquery, M., Lepage, H., Gairoard, S., Gattacceca, J.C., Ambrosi, J.-P., Radakovitch, O., 2018. Observatoire des Sédiments du Rhône. INRAE. https://doi.org/10.17180/OBS.OSR.
Tolosana-Delgado, R., 2012. Uses and misuses of compositional data in sedimentology. Sedim. Geol., Actualist. Models Sedim. Generat. 280, 60–79. https://doi.org/10.1016/j.sedgeo.2012.05.005.
Van Metre, P.C., Mesnage, V., Laignel, B., Motelay, A., Deloffre, J., 2008. Origins of sediment-associated contaminants to the Marais Vernier, the Seine Estuary, France. Water Air Soil Pollut. 191, 331–344. https://doi.org/10.1007/s11270-008-9628-9.
Vane, C.H., Turner, G.H., Chenery, S., Richardson, M., Cave, M.C., Terrington, R., Gowing, C.J.B., Moss-Hayes, V., 2020. Trends in heavy metals, polychlorinated biphenyls and toxicity from sediment cores of the inner River Thames estuary, London, UK. Environ. Sci. Processes Impacts 22, 364–380. https://doi.org/10.1039/C9EM00430K.
Vauclin, S., Mourier, B., Piégay, H., Winiarski, T., 2020. Legacy sediments in a European context: The example of infrastructure-induced sediments on the Rhône River. Anthropocene 31, 100248. https://doi.org/10.1016/j.ancene.2020.100248.
Vauclin, S., Mourier, B., Tena, A., Piégay, H., Winiarski, T., 2019. Effects of river infrastructures on the floodplain sedimentary environment in the Rhône River. J Soils Sedim. https://doi.org/10.1007/s11368-019-02449-6.
Vernet, J.-P., Viel, M., 1984. Métaux lourds dans les sédiments lacustres. In: Le Léman, synthèse 1957–1982. CIPEL, Lausanne, pp. 227–238.
Vrel, A., 2012. Reconstitution de l'historique des apports en radionucléides et contaminants métalliques à l'estuaire fluvial de la Seine par l'analyse de leur enregistrement sédimentaire (PhD Thesis). Université de Caen, Caen.
Wessels, M., Lenhard, A., Giovanoli, F., Bollhöfer, A., 1995. High resolution time series of lead and zinc in sediments of Lake Constance. Aquat. Sci. 57, 291–304. https://doi.org/10.1007/BF00878394.
WFD AMPS, 2004. Discussion document on sediment monitoring guidance for the EU Water Framework Directive. Working Group on Analysis and Monitoring of Priority Substances.
Wickham, H., Chang, W., Henry, L., Pedersen, T.L., Takahashi, K., Wilke, C., Woo, K., 2019. Package 'ggplot2'. Create Elegant Data Visualisations Using the Grammar of Graphics. Version 3.1.1.
Wildi, W., Dominik, J., Loizeau, J.-L., Thomas, R.L., Favarger, P.-Y., Haller, L., Perroud, A., Peytremann, C., 2004. River, reservoir and lake sediment contamination by heavy metals downstream from urban areas of Switzerland. Lakes Reserv.: Sci. Policy Manage. Sustain. Use 9, 75–87. https://doi.org/10.1111/j.1440-1770.2004.00236.x.
Wildi, W., Koukal, B., Ischi, V., Perroud, A., 2006. Qualité des sédiments de la retenue de Verbois; comparaison avec les sédiments des rivières suisses et du Léman. Archives des Sciences 59, 131–140.
Winfield, M., Jamison, A., Wong, R., Czajkowski, P., 2006. Nuclear Power in Canada: An Examination of Risks, Impacts and Sustainability. The Pembina Instute, Calgary, Canada.
Wood, S., 2019. Package 'mgcv'. Mixed GAM Computation Vehicle with Automatic Smoothness Estimation. Version 1.8-28.
Zhang, W., Feng, H., Chang, J., Qu, J., Xie, H., Yu, L., 2009. Heavy metal contamination in surface sediments of Yangtze River intertidal zone: An assessment from different indexes. Environ. Pollut., Special Issue Sect.: Ozone Mediterranean Ecol.: Plants, People, Problems 157, 1533–1543. https://doi.org/10.1016/j.envpol.2009.01.007.